

# Adaptive Model Predictive Control

Denis Koksal-Rivet

February 2019



## DECLARATION OF AUTHORSHIP

You should complete this certificate. It should be bound into your fourth year project report, immediately after your title page. Three copies of the report should be submitted to the Chairman of examiners for your Honour School, c/o Clerk of the Schools, examination Schools, High Street, Oxford.

Name (in capitals): .....

College (in capitals): ..... Supervisor: .....

Title of project (in capitals): .....

Page count (excluding risk and COSHH assessments): .....

Please tick to confirm the following:

I have read and understood the University's disciplinary regulations concerning conduct in examinations and, in particular, the regulations on plagiarism (*The University Student Handbook. The Proctors' and Assessors' Memorandum, Section 8.8*; available at <https://www.ox.ac.uk/students/academic/student-handbook>) ☐

I have read and understood the Education Committee's information and guidance on academic good practice and plagiarism at <https://www.ox.ac.uk/students/academic/guidance/skills>. ☐

The project report I am submitting is entirely my own work except where otherwise indicated. ☐

It has not been submitted, either partially or in full, for another Honour School or qualification of this University (except where the Special Regulations for the subject permit this), or for a qualification at any other institution. ☐

I have clearly indicated the presence of all material I have quoted from other sources, including any diagrams, charts, tables or graphs. ☐

I have clearly indicated the presence of all paraphrased material with appropriate references. ☐

I have acknowledged appropriately any assistance I have received in addition to that provided by my supervisor. ☐

I have not copied from the work of any other candidate. ☐

I have not used the services of any agency providing specimen, model or ghostwritten work in the preparation of this project report. (See also section 2.4 of Statute XI on University Discipline under which members of the University are prohibited from providing material of this nature for candidates in examinations at this University or elsewhere: <http://www.admin.ox.ac.uk/statutes/352-051a.shtml>.) ☐

The project report does not exceed 50 pages (including all diagrams, photographs, references and appendices). ☐

I agree to retain an electronic copy of this work until the publication of my final examination result, except where submission in hand-written format is permitted. ☐

I agree to make any such electronic copy available to the examiners should it be necessary to confirm my word count or to check for plagiarism. ☐

Candidate's signature: .....

Date: .....

### Abstract

This report examines existing robust adaptive model predictive controller algorithms found in the current literature and presents novel improvements to the existing algorithms. The discussion of these existing algorithms is based largely on the work of Lu and Cannon [1]. The robust tube based MPC algorithm presented in the literature formulates the state tube in H-form, which requires the calculation of the parameter set estimate in V-form online, which is computationally expensive. To overcome this expensive computation the current algorithm restricts the parameter set estimate to be a hypercube so that the computation of the V-form is easy. This is in general a restrictive shape for the parameter set estimate and is not guaranteed to model the parameter set precisely. To overcome this restriction, this report proposes a computationally tractable, equivalent conversion between H-form and V-form representations of the state tube. This conversion to a V-form representation of the state tubes means that the calculation of the V-form of the parameter set estimate is no longer required, allowing the shape of the parameter set estimate to be arbitrarily complex, meaning that more accurate estimations for the parameter set can be achieved. Another significant motivation of the V-form algorithm is the ease of implementation of a persistent excitation condition at each time step of the online optimisation. This report proposes a novel persistent excitation condition which considers future predicted time steps.

Matlab simulations of the existing H-form algorithm and the newly proposed V-form algorithm are presented, and it is shown that the results are comparable as expected. Simulations of the V-form algorithm with the newly proposed future persistent excitation condition are also presented, and it is shown that the implementation of this condition results in significantly faster convergence of the parameter set estimate compared to the existing algorithm.

The report also proposes a modification of the proposed V-form algorithm, where the parameter set update section of the algorithm is reformulated to allow convergence of the parameter set update to the true parameter value  $\theta^*$  even in the presence noise, where the system parameter value at time step  $k$  is given by  $\theta_k = \theta^* + \tilde{\theta}_k$ , where  $\tilde{\theta}_k \in S = \{\theta : U\theta \leq h\}$ . Simulations of this modification show that the parameter set estimate converges to a singleton containing the value of  $\theta^*$ , and a proof is given that guarantees this result over a long enough simulation.

### Acknowledgements

I would like to express my deep gratitude to Prof Mark Cannon as this report would not have been possible without his valuable support, recommendations, and insights. His willingness to give his time, enthusiasm, and thorough explanations of complex topics are greatly appreciated.

I also wish to thank my parents for their continued support and encouragement throughout the course of this project.

# Contents

<b>1</b>	<b>Introduction</b>	<b>5</b>
<b>2</b>	<b>Notation</b>	<b>5</b>
<b>3</b>	<b>Tube Based Model Predictive Control Algorithm</b>	<b>6</b>
3.1	Polytopic Tubes for Constraint Satisfaction . . . . .	7
3.2	Design of $V$ and $K$ . . . . .	8
3.3	Computing the Optimal Input . . . . .	9
<b>4</b>	<b>Model Identification</b>	<b>9</b>
4.1	Set Based Model Identification . . . . .	10
4.2	Point Estimate . . . . .	11
4.3	Parameter Set Convergence . . . . .	12
4.3.1	Rate of Parameter Set Convergence . . . . .	16
<b>5</b>	<b>Persistent Excitation</b>	<b>16</b>
5.1	Convex Sufficient Condition for Persistent Excitation . . . . .	16
<b>6</b>	<b>Implementation</b>	<b>18</b>
6.1	Existing MPC Algorithm [1] . . . . .	18
6.2	H-form Implementation . . . . .	22
6.3	V-form Implementation . . . . .	27
6.3.1	Calculation of $\mathcal{R}_j$ and $U^j$ . . . . .	31
6.4	Comparing H-Form and V-Form Implementations . . . . .	33
6.5	Improvements on Existing Algorithms . . . . .	36
6.5.1	Future Persistent Excitation Condition . . . . .	36
6.5.2	Varying True Model Parameter . . . . .	39
<b>7</b>	<b>Results and Discussion</b>	<b>41</b>
7.1	Future PE Condition . . . . .	41
7.2	Varying True Model Parameter . . . . .	48
<b>8</b>	<b>Conclusions</b>	<b>52</b>

## 1 Introduction

Starting from the 1960s onward, advanced process control techniques have been of particular interest in both academia and industry. Early versions of model predictive control algorithms were first developed in the 1970s independently by Cutler and Ramaker at Shell Oil and Jacques Richalet [2]. These control methods were first developed in the process and petrochemical industries and improved controller performance compared to PID controllers that were being used at the time. Based on the success of the predictive control methods, MPC algorithms have become the most common advanced control methodology in use in industry today.

Model predictive control is an optimal control strategy that relies on numerical optimisation where future control inputs and plant responses are predicted using a system model and optimised with regards to a performance index. MPC has become a pervasive control methodology due to its ease of implementation, ability to scale to large problems, concrete stability, optimality, and robustness properties, and systematic method for dealing with input and state constraints [3].

The performance of model predictive controllers is strongly dependent upon the quality of the underlying model as inaccurate models lead to poor predictions and thus poor control of the plant. Stochastic and robust MPC approaches have commanded a lot of attention in the relevant literature as these methods deal effectively with unmodeled dynamics and quickly changing disturbances, but are inherently conservative in problems with slow changing or constant parametric uncertainty [4]. Bounds on the performance of MPC laws have led to developments that combine adaptive control with MPC which have led to decreased conservativeness compared to robust MPC without sacrificing robust stability guarantees. The recent literature on adaptive MPC examines several methods for parameter identification such as comparison sets, set membership identification, recursive least squares, and neural networks. Set membership identification techniques describe a set that the true parameters of the model lie in which in turn defines a set of possible plant models, and then enforces that constraints are satisfied on all plant models within this set [1].

## 2 Notation

Integers and reals will be denoted by  $\mathbb{N}$  and  $\mathbb{R}$  respectively, and  $\mathbb{N}_{\geq 0} = \{n \in \mathbb{N} : n \geq 0\}$ , and more generally  $\mathbb{N}_{[a,b]} = \{n \in \mathbb{N} : a \leq n \leq b\}$ . The  $i^{\text{th}}$  row of a matrix and  $i^{\text{th}}$  element of a vector will be represented as  $[A]_i$  and  $[a]_i$ .  $\max_{x \in \mathbb{X}} J(x)$  will denote the maximum value of  $J$  over the set  $\mathbb{X}$  while  $[x]_{\geq 0} = \max\{0, x\}$ . The inequality  $A \geq B$  will be taken to represent an element wise inequality whereas  $A \succeq B$  will mean  $x^T A x \geq x^T B x$  for all vectors  $x$  and square matrices  $A$  and  $B$ . Finally, the

prediction for the variable  $z$   $k$  steps ahead, predicted at time  $t$ , will be indicated by  $z_{k|t}$  [1].

### 3 Tube Based Model Predictive Control Algorithm

Cannon and Lu [1] consider state space systems and implement set-based model identification and robust tube MPC. This section will review the adaptive MPC approach used in this paper. The system considered is a linear system with linear constraints on states and inputs, with an unknown additive disturbance term.

$$x_{t+1} = A(\theta)x_t + B(\theta)u_t + w_t \quad (1)$$

The system matrices  $A(\theta)$  and  $B(\theta)$  depend on an unknown parameter  $\Theta$  through the relationship given in equation 2, where the matrices  $(A_i, B_i)$  for  $i = 0, 1, \dots, p$  are assumed to be known.

$$(A(\theta), B(\theta)) = (A_0, B_0) + \sum_{i=1}^p (A_i, B_i)[\theta]_i \quad (2)$$

The constraints on the state and inputs are expressed as

$$Fx_t + Gu_t \leq \mathbf{1} \quad \forall t \in \mathbb{N}_{\geq 0} \quad (3)$$

and the unknown additive disturbance lies in the convex polytopic set  $\mathbb{W}$  where

$$\mathbb{W} = \{w : \Pi_w w \leq \pi_w\} \quad (4)$$

with  $\pi_w \geq 0$ . An initial estimate of the parameter set is given by  $\Theta_0$  and it is assumed to contain the true parameter value. A simplifying assumption that  $\Theta_0 = \{\theta : \Pi_\theta \theta \leq \pi_\theta\}$  takes the form of a zonotope ( $\Pi_\theta^T = [\Pi^T \quad -\Pi^T]$ ) is made in order to restrict the complexity of the shape of the parameter set. As in many MPC formulations the predicted control sequences have the dual form:

$$u_{k|t} = \begin{cases} Kx_{k|t} + v_{k|t}, & \forall k \in \mathbb{N}_{[0, N-1]} \\ Kx_{k|t}, & \forall k \geq N \end{cases} \quad (5)$$

The objective is thus to solve an optimal regulation problem to ensure stability of the closed-loop system while ensuring that the constraints in equation 3 are satisfied at each time step, given knowledge of  $\mathbb{W}$  and  $\Theta_0$ . The paper also pursues the additional objective of updating the set  $\Theta_t$  using state measurements and using the updated parameter set to improve the controller performance, the details of which will be discussed later in this report.

The paper makes the assumption that there exists a polytopic set  $\mathbb{X} = \{x : Vx \leq \mathbf{1}\}$  and feedback gain  $K$  so that  $\mathbb{X}$  is  $\lambda$ -contractive for some  $\lambda \in [0, 1)$ , which is equivalent to the system (1) being robustly stabilisable for all  $\theta \in \Theta_0$  :

$$V(A(\theta) + B(\theta)K)x \leq \lambda \mathbf{1} \quad \forall x \in \{x : Vx \leq \mathbf{1}\} \text{ and } \theta \in \Theta_0 \quad (6)$$

The matrices  $V$  and  $K$  are designed offline [1].

### 3.1 Polytopic Tubes for Constraint Satisfaction

This section examines the robust tube MPC algorithm of [1] which constructs a sequence of polytopic sets that bound the evolution of the state of the uncertain system (1). The algorithm then ensures the satisfaction of system constraints at each state lying in these polytopic sets. The predicted tube for the state  $x$  at time  $k$  is defined as  $\mathbb{X}_k = \{x : Vx \leq \alpha_k\}$ . At each time step, a tube, consisting of a sequence of sets  $\mathbb{X}_0, \mathbb{X}_1, \dots, \mathbb{X}_{N-1}$  is constructed that satisfy

$$\Phi(\theta)x + B(\theta)v_k + w \in \mathbb{X}_{k+1} \quad \forall x \in \mathbb{X}_k, w \in \mathbb{W}, \theta \in \Theta \quad (7)$$

where  $\Phi(\theta) = A(\theta) + B(\theta)K$ . For  $x_k \in \mathbb{X}_k$  and  $u_k = Kx_k + v_k$ , the constraints (3) are satisfied for the  $k$ th prediction time step if

$$H_c \alpha_k + Gv_k \leq \mathbf{1} \quad (8)$$

where  $H_c$  is computed offline by solving the linear program below.

$$[H_c]_i = \underset{H \in \mathbb{R}^{1 \times n_\alpha}}{\operatorname{argmin}} H \mathbf{1} \quad \text{s.t. } H \geq 0, HV = [F + GK]_i \quad \text{for each } i \in \mathbb{N}_{[1, n_c]} \quad (9)$$

The proof is as follows: the constraints (3) are satisfied for  $x_k \in \mathbb{X}_k$  and  $u_k = Kx_k + v_k$  if,

$$(F + GK)x + Gv_k \leq \mathbf{1} \quad (10)$$

for all  $x \in \mathbb{X}_k$ , which can be expressed as  $\{x : Vx \leq \alpha_k\} \subseteq \{x : (F + GK)x \leq \mathbf{1} - Gv_k\}$ . Using proposition 3.31 from [5], this statement is equivalent to there being a matrix  $H_c$  such that  $H_c \geq 0$ ,  $H_c V = F + GK$ ,  $H_c \alpha_k + Gv_k \leq \mathbf{1}$ , and  $H_c$  satisfying these conditions can be computed by solving the linear program in equation 9. Furthermore, constraint (7) is satisfied if

$$\hat{\theta}^T \hat{H}_i \alpha_k + [V]_i B(\theta^{(j)}) v_k + \bar{w}_i \leq [\alpha_{k+1}]_i \quad (11)$$

for all  $j = 1, \dots, m$  and  $i = 1, \dots, n_\alpha$  where  $\bar{w}_i = \max_{w \in \mathbb{W}} [V]_i w$ ,  $\hat{\theta}^{(j)T} = [1 \ \theta^{(j)T}]$  ( $\theta^{(j)}$  is the  $j$ th vertex of the parameter set estimate such that  $\theta \in \Theta = \text{co}\{\theta^{(1)}, \dots, \theta^{(m)}\}$ ), and the matrices  $\hat{H}_i$  are computed offline as the solution of the following linear program for each  $i = 1, \dots, n_\alpha$ .

$$\begin{aligned} \hat{H}_i = & \underset{H \in \mathbb{R}^{(p+1) \times n_\alpha}}{\text{argmin}} \max_{j \in \mathbb{N}_{[1, m]}} \hat{\theta}^{(j)T} H \mathbf{1} \\ \text{s.t. } & \hat{\theta}^{(j)T} H \geq 0, \ j \in \mathbb{N}_{1, m}, \ HV = \begin{bmatrix} [V]_i \Phi_0 \\ \vdots \\ [V]_i \Phi_p \end{bmatrix} \end{aligned} \quad (12)$$

The proof of this follows along similar lines to the previous proof: The condition of satisfaction of (7) is equivalent to  $\{x : Vx \leq \alpha_k\} \subseteq \{x : V\Phi(\theta)x + VB(\theta)v_k + \bar{w} \leq \alpha_{k+1}\}$ . Again, by proposition 3.31 in [5], this is equivalent to the following conditions being satisfied:

$$\hat{\theta}^{(j)T} \hat{H}_i \geq 0 \quad (13)$$

$$\hat{H}_i V = [[V]_i \Phi_0 \ \dots \ [V]_i \Phi_p]^T \quad (14)$$

$$\hat{\theta}^{(j)T} \hat{H}_i \alpha_k + [V]_i B(\theta^{(j)})v_k + \bar{w} \leq [\alpha_{k+1}]_i \quad (15)$$

(13) and (14) are computed offline by solving the LP in equation 12 for each  $i \in \mathbb{N}_{[1, n_\alpha]}$ . Thus, constraint (15) is enough to ensure satisfaction of the constraint (7). The initial and final conditions on the state tubes are imposed through the conditions below.

$$\alpha_0 \geq Vx \quad (16)$$

$$[\alpha_N]_i \geq \hat{\theta}^{(j)T} \hat{H}_i \alpha_N + \bar{w}, \ \forall j = 1, \dots, m \text{ and } i = 1, \dots, n_\alpha \quad (17)$$

$$H_c \alpha_N \leq \mathbf{1} \quad (18)$$

### 3.2 Design of $V$ and $K$

As the matrix  $V$  defines the tube cross section  $\mathbb{X}_k$  at every time step, increasing the number of rows,  $n_\alpha$ , in  $V$  will result in tighter bounds on the predicted state tube. However, there is a trade off that has to be considered, as increasing  $n_\alpha$  increases the dimensions of many of the matrices involved in the online optimisation, thus greatly increasing the computation needed to compute an optimal solution at each time step.

For a given  $V$ , the  $\lambda$  value that satisfies the  $\lambda$ -contractivity condition (6) is found by minimising  $\lambda$  subject to  $\{x : Vx \leq \mathbf{1}\} \subseteq \{x : V\Phi(\theta)x \leq \lambda \mathbf{1}\}$ . When  $V$  is chosen independently of  $K$  this



optimisation is linear with respect to  $K$  and  $\lambda$ . Computing  $V$  simultaneously with  $K$  would involve solving a non-convex optimisation; this choice of  $V$  is a convenient heuristic, and hence is not optimal, but will make the optimisation convex.  $V$  should be chosen as  $V = [Q^T \ F_0^T]^T$  where  $F_0$  is the rows of  $F$  where the corresponding rows of  $G$  are equal to 0, and  $Q$  is chosen so that the set  $x : Qx \leq 1$  is a polytopic approximation of an ellipsoidal Lyapunov function for the model (1) with control law  $u_k = Kx_k$ ; this Lyapunov function can be computed by solving a semidefinite program. Again using proposition 3.31 from [5], the calculation of  $K$  is reduced to solving the LP problem below [1].

$$\begin{aligned}
(\lambda, K, \hat{H}_1, \dots, \hat{H}_{n_\alpha}) &= \underset{\lambda, K, \hat{H}_1, \dots, \hat{H}_{n_\alpha}}{\operatorname{argmin}} \lambda \\
\text{s.t. } \lambda &\geq \hat{\theta}^{(j)T} \hat{H}_i \mathbf{1}, \quad \hat{\theta}^{(j)T} \hat{H}_i \geq 0 \quad \forall j = 1, \dots, m, \quad i = 1, \dots, n_\alpha \\
\hat{H}_i V &= [[V]_i(A_0 + B_0 K) \quad \dots \quad [V]_i(A_p + B_p K)]^T
\end{aligned} \tag{19}$$

### 3.3 Computing the Optimal Input

Having set out all of the constraints for the tube based MPC problem, the online optimisation to compute the optimal input at each time step can now be formulated. The online optimisation minimises a given cost  $J(x, u)$  with respect to the constraints discussed in the previous section.  $J(x, u)$  is a performance index that is constructed to penalise deviations from the desired steady state values of  $x$  and  $u$ . More formally, the online MPC algorithm is as follows:

$$\begin{aligned}
J^o &= \min_{\mathbf{v}, \boldsymbol{\alpha}} J(x, u) \\
\text{s.t. } H_c \alpha_k + G v_k &\leq \mathbf{1} \\
\alpha_0 &\geq Vx \\
[\alpha_N]_i &\geq \hat{\theta}^{(j)T} \hat{H}_i \alpha_N + \bar{w}, \quad \forall j = 1, \dots, m \text{ and } i = 1, \dots, n_\alpha \\
H_c \alpha_N &\leq \mathbf{1} \\
\hat{\theta}^{(j)T} \hat{H}_i \alpha_k + [V]_i B(\theta^{(j)}) v_k + \bar{w} &\leq [\alpha_{k+1}]_i
\end{aligned} \tag{20}$$

where the sequences  $\boldsymbol{\alpha} = \{\alpha_0, \alpha_1, \dots, \alpha_N\}$  and  $\mathbf{v} = \{v_0, v_1, \dots, v_{N-1}\}$  are the optimisation variables [1].

## 4 Model Identification

This section will discuss methods for set based model identification, examine a Least Mean Squares method for deriving a point estimate for the model parameter, and explore the relevant theory on

the rate of parameter set convergence. Model identification is an important component of the entire MPC algorithm explored in this report as the performance of the controller discussed in the previous section improves greatly as the model becomes more accurate.

#### 4.1 Set Based Model Identification

The discussion in [1] of set based model identification is derived from the theory explained in [6] and [7]. Observations of the system states and control inputs are used online to construct a polytope that the possible model parameters could lie in. This is called the unfalsified parameter set and it is combined with the current polytopic parameter set estimate to construct the new parameter set estimate. The unfalsified parameter set is defined at time  $t$  as

$$\begin{aligned}\Delta_t &= \{\theta : x_t - (A(\theta)x_{t-1} + B(\theta)u_{t-1}) \in \mathbb{W}\} \\ &= \{\theta : -\Pi_w D(x_{t-1}, u_{t-1})\theta \leq \pi_w + \Pi_w d_t\} \\ &= \{\theta : P_t \theta \leq Q_t\}\end{aligned}\tag{21}$$

where  $P_t = -\Pi_w D(x_{t-1}, u_{t-1})$  and  $Q_t = \pi_w + \Pi_w d_t$ .  $D(x, u)$  and  $d_t$  are defined according to the equations below.

$$D(x, u) = \begin{bmatrix} A_1 x + B_1 u & \dots & A_p x + B_p u \end{bmatrix}\tag{22}$$

$$d_t = A_0 x_{t-1} + B_0 u_{t-1} - x_t\tag{23}$$

For the parameter set update algorithm,  $\Pi_\theta$  is a matrix chosen beforehand that defines the initial parameter set  $\Theta_0 = \{\theta : \Pi_\theta \theta \leq \pi_0\}$ , and at each subsequent time step the parameter set is defined by  $\Theta_t = \{\theta : \Pi_\theta \theta \leq \pi_t\}$  where  $\pi_t$  is determined online by the parameter set update algorithm. The complexity of the parameter set can be controlled by choosing  $\Pi_\theta$  appropriately, and it is common to define the parameter set to be a hypercube by defining  $\Pi_\theta = [I \quad -I]^T$ . The smallest set  $\Theta_{t+1}$  of the form  $\Theta_{t+1} \supseteq \Theta_t \cap \Delta_t$  is obtained by solving the linear program below for  $i = 1, \dots, 2n$ . If  $\Pi_\theta \theta \leq \pi_0$  and  $\pi_{t+1}$  is found by solving the LP (24), then  $\Theta_t \supseteq \Theta_{t+1} \supseteq \Theta_t \cap \Delta_t$ , i.e. the parameter set is not expanding.  $\pi_{t+1}$  also defines the minimum volume set of the form  $\{\theta : \Pi_\theta \theta \leq \pi_{t+1}\}$  containing the union of  $\Theta_t$  and  $\Delta_t$ . The proof is as follows: The constraints in equation 24 necessarily ensure that  $\Theta_{t+1} \supseteq \Theta_t \cap \Delta_t$ , implying by induction that  $\theta \in \Theta_t$  for all  $t$ .  $H_i = [\mathbb{I} \quad 0]$  and  $\pi_{t+1} = \pi_t$  provide a feasible solution for (24), so it must follow that  $\pi_{t+1} \leq \pi_t$  and thus  $\Theta_{t+1} \subseteq \Theta_t$  for all  $t$ . The volume of  $\Theta_{t+1}$  is given by  $(2_p / \det(\Pi_\theta)) \prod_{i=1}^p ([\pi_{t+1}]_i + [\pi_{t+1}]_{p+1})$  which is minimised for any  $\Pi_\theta$  by the choice of objective function in equation 24 [1].

$$\begin{aligned}
[\pi_{t+1}]_i &= \min_{\pi, H_i} \pi \\
\text{s.t. } H_i \begin{bmatrix} \Pi_\theta \\ P_t \end{bmatrix} &= [\Pi_\theta]_i \\
H_i \begin{bmatrix} \pi_t \\ Q_t \end{bmatrix} &\leq \pi \\
H_i &\geq 0
\end{aligned} \tag{24}$$

## 4.2 Point Estimate

A point estimate method for the unknown model parameters  $\theta$  can be used in conjunction with the set-based model identification algorithm discussed previously to ensure a finite closed-loop gain from the additive disturbance to the system state  $x_k$  [4]. In order to provide this stability guarantee between the disturbance and state, a Least Mean Squares filter is used. Hassibi et al. have shown in [8] that the LMS filter is an  $H_\infty$  optimal map from the disturbance sequence to the sequence of prediction errors, resulting in a finite gain between the disturbance and the state prediction error. The point estimate algorithm is as follows: given an estimate for the model parameters,  $\hat{\theta}_k$ , define the predicted state to be  $\hat{x}_{1|k} = A(\hat{\theta}_k)x_k + B(\hat{\theta}_k)u_k$  and the prediction error is thus denoted as  $\tilde{x}_{1|k} = A(\theta^*)x_k + B(\theta^*)u_k - \hat{x}_{1|k}$ , where  $\theta^*$  represents the true parameter value. For a given initial estimate of the parameters,  $\hat{\theta}_0 \in \Theta$  and a parameter update gain  $\mu$  satisfying  $\frac{1}{\mu} > \sup_{(x,\mu)} \|D(x,\mu)\|^2$ , the estimate is defined recursively according to the equations below.

$$\begin{aligned}
\tilde{\theta}_k &= \hat{\theta}_{k-1} + \mu D(x_{k-1}, u_{k-1})^T (x_k - \hat{x}_{1|k-1}) \\
\hat{\theta}_k &= \Pi_{\Theta_k}(\tilde{\theta}_k)
\end{aligned} \tag{25}$$

$\Pi_\Theta(\tilde{\theta})$  represents the Euclidean projection of a point  $\tilde{\theta} \in \mathbb{R}^p$  onto the set  $\Theta$  and is calculated as  $\Pi_\Theta(\tilde{\theta}) = \operatorname{argmin}_{\theta \in \Theta} \|\theta - \tilde{\theta}\|$ . This point estimate then results in the aforementioned guarantee about the closed-loop gain from disturbance to system state. If  $\sup_k \|x_k\| < \infty$ ,  $\sup_k \|u_k\| < \infty$ , then  $\hat{\theta}_k$  is bounded ( $\hat{\theta}_k \in \Theta$ ) and

$$\sup_{m \in \mathbb{N}, w_k \in \mathbb{W}, \hat{\theta}_0 \in \Theta} \frac{\sum_{k=0}^m \|\tilde{x}_{1|k}\|^2}{\frac{1}{\mu} \|\hat{\theta}_0 - \theta^*\|^2 + \sum_{k=0}^m \|w_k\|^2} \leq 1 \quad [4]. \tag{26}$$

The boundedness of  $\hat{\theta}_k$  and  $\hat{\theta}_k \in \Theta$  follow trivially from equation (21) and projection. The proof for

equation (26) is not as trivial; the proof is as follows:

$$\begin{aligned}
& \frac{1}{\mu} \|\hat{\theta}_{k+1} - \theta^*\|^2 - \frac{1}{\mu} \|\hat{\theta}_k - \theta^*\|^2 \\
& \leq \frac{1}{\mu} \|\tilde{\theta}_{k+1} - \theta^*\|^2 - \frac{1}{\mu} \|\hat{\theta}_k - \theta^*\|^2 \\
& = \frac{1}{\mu} \|\tilde{\theta}_{k+1} - \hat{\theta}_k\|^2 + \frac{2}{\mu} (\tilde{\theta}_{k+1} - \hat{\theta}_k)^T (\hat{\theta}_k - \theta^*) \\
& = \frac{1}{\mu} \|\mu D_k^T (\tilde{x}_{1|k} + w_k)\|^2 + 2(\tilde{x}_{1|k} + w_k)^T D_K (\hat{\theta}_k - \theta^*) \\
& \leq (\mu \|D_k\|^2 - 1) \|\tilde{x}_{1|k} + w_k\|^2 - \|\tilde{x}_{1|k}\|^2 + \|w_k\|^2 \\
& \leq -\|\tilde{x}_{1|k}\|^2 + \|w_k\|^2
\end{aligned} \tag{27}$$

where  $D_k = D(x_k, u_k)$ . The first inequality is due to the projection operator being non-expansive and  $\theta^* \in \Theta$ . Equation 25 is used in the second half of (27) along with a completion of squares, using the identities  $x_{k+1} - \hat{x}_{1|k} = \tilde{x}_{1|k} + w_k$ ,  $\tilde{x}_{1|k} = D_k(\theta^* - \hat{\theta}_k)$ . Summing 27 from  $k = 0$  to  $m$  gives

$$\frac{1}{\mu} \|\hat{\theta}_{m+1} - \theta^*\|^2 + \sum_{k=0}^m \|\tilde{x}_{1|k}\|^2 \leq \sum_{k=0}^m \|w_k\|^2 + \frac{1}{\mu} \|\hat{\theta}_0 - \theta^*\|^2 \tag{28}$$

which proves the claim above. As a result, the prediction error converges to 0 asymptotically if  $\sup_k \|x_k\|^2 < \infty$ ,  $\sup_k \|u_k\|^2 < \infty$ , and  $\sum_{k=0}^{\infty} \|w_k\|^2 < \infty$  [4].

### 4.3 Parameter Set Convergence

Having defined the set membership based technique for model identification, it is important to examine the properties of this membership set, chiefly whether it converges to the true parameters and how fast it converges. Bai, Cho, and Tempo's paper [9] provides a thorough examination of the bounded-error parameter estimation approach making use of some probabilistic assumptions. The choice of noise model is very important for parameter identification, and several different models are discussed in [9]. For conciseness, only the pointwise bound noise model will be discussed in this report, but the interested reader is directed to [9] for a more complete discussion surrounding different types of noise models.

A pointwise bound noise model is defined as

$$\mathbb{W} = \{w : \max_{1 \leq i \leq N} |w_i| \leq \epsilon\}, \tag{29}$$

where  $w_i$  refers to the  $i$ th element of the disturbance vector  $w$  and  $N$  refers to the size of the disturbance vector.  $N$  will refer to the size of the disturbance vector  $w$  for the rest of Section 4.3, as opposed to

the prediction horizon length, as it does in the rest of this report. This model fits the assumptions made in previous sections that  $w_k$  ( $w_k$  being the disturbance vector  $w$  at time  $k$ ) belongs to a bounded polytopic set. This can be seen by reformulating (29) as  $-\epsilon \leq w_i \leq \epsilon$  for  $i = 1, \dots, N$ , meaning that the disturbance  $w_k$  lies in a hypercube of  $N$  dimensions, centred on the origin and with side length of  $2\epsilon$ . For a system defined by  $y = \Phi\theta + \nu$  where  $\Phi$  is the regressor and  $\nu$  is the additive noise, the membership set (parameter set estimate) can be identified by the equation

$$S_N^p = \cap_{i=1}^N \{\hat{\theta} : |y_i - \phi_i^T \hat{\theta}| \leq \epsilon\}. \quad (30)$$

The system (1) considered in this report can be reformulated in this form by writing  $x_{t+1} = A(\theta)x_t + B(\theta)u_t + w_t = A_0x_t + A_1[\theta]_1x_t + A_2[\theta]_2x_t + A_3[\theta]_3x_t + B_0u_t + B_1[\theta]_1u_t + B_2[\theta]_2u_t + B_3[\theta]_3u_t + w_t = [A_1x_t + B_1u_t \ A_2x_t + B_2u_t \ A_3x_t + B_3u_t]\theta + A_0x_t + B_0u_t + w_t$ , from which it is easy to see  $\Phi = [A_1x_t + B_1u_t \ A_2x_t + B_2u_t \ A_3x_t + B_3u_t]$ . The motivation for constructing the membership set is due to the fact that given an estimate for the model parameters  $\hat{\theta}$  and the presence of noise, it is generally not possible to know whether the estimate coincides with the true parameters, but it is possible to determine whether the estimate for the parameters is consistent with observed input-output data. To evaluate the quality of parameter estimation, the diameter of the membership set is defined as

$$\text{dia}S_N^p = \sup_{\theta_1, \theta_2 \in S_N^p} \|\theta_1 - \theta_2\|_2, \quad (31)$$

with the 2-norm being used to simplify the calculation. The volume of the membership set is also often used in the literature as a quantitative measure of parameter estimation, but a zero-volume membership set does not necessarily imply zero error in the parameter estimation, and thus this report will make use of the membership set diameter when evaluating parameter estimation error. A small membership set diameter implies small uncertainty in the parameter estimate, and if the diameter is zero, the membership set is a singleton consisting of the true parameter value.

Bai et al. show that, if the noise is assumed to be a sequence of random variables, the diameter of the membership set converges. The assumption that the noise is a random variable is not necessarily straightforward. In cases where a significant portion of the noise is due to under-modelling, the assumption will not hold, and probabilistic guarantees about the convergence of the membership set diameter cannot be made. The discussion around the guarantee of diameter convergence must first begin with the definition of tightness of the noise bound. For the pointwise bound noise model, a bound  $\epsilon$  on the random noise variable  $w_i$  is said to be tight if there is a non-zero probability that the

value of  $w_i$  lies on the boundary at  $-\epsilon$  or  $\epsilon$ . More formally, for any  $\rho > 0$  and each  $i$

$$\text{Prob}\{-\epsilon \leq w_i \leq -\epsilon + \rho\} \geq p_1(\rho) > 0 \quad (32)$$

and

$$\text{Prob}\{\epsilon - \rho \leq w_i \leq \epsilon\} \geq p_1(\rho) > 0 \quad (33)$$

for some  $1 > p_1(\rho) > 0$ .

For the system being considered with a pointwise noise model, the diameter of the membership set converges to zero as  $N \rightarrow \infty$  with probability of 1 if the noise sequence  $\{w_i\}$  is a sequence of random variables and the bound  $\epsilon$  is tight, and the regressor of the system is persistently exciting. The regressor  $\phi_i$  is persistently exciting if

$$\beta^2 I \preceq \frac{1}{m} \sum_{i=i_0+1}^{i_0+m} \phi_i \phi_i^T \preceq \alpha^2 I \quad (34)$$

for some  $\alpha, \beta, m > 0$  and all  $i_0$ . The upper bound is automatically satisfied if the system is stable and the input and noise are bounded. The proof is rather convoluted, but summarised next for completeness.

Let  $\hat{\theta}$  be any arbitrary fixed point not equal to the true parameter value  $\theta^*$ . To show that  $\hat{\theta}$  is excluded from  $S_N^p(\epsilon)$  in probability as  $N \rightarrow \infty$ , define

$$z_k = \max\left\{\frac{1}{m} \sum_{i=1}^m (y_i - \phi_i^T \hat{\theta})^2, \frac{1}{m} \sum_{i=m+1}^{2m} (y_i - \phi_i^T \hat{\theta})^2, \dots, \frac{1}{m} \sum_{i=(k-1)m+1}^{km} (y_i - \phi_i^T \hat{\theta})^2\right\}. \quad (35)$$

It is enough to show that  $\text{Prob}\{z_k > \epsilon^2\} \rightarrow 1$  as  $k \rightarrow \infty$ . Given  $\tilde{\theta} = \theta - \hat{\theta}$  and  $\phi_i$  is persistently exciting, the following equation is true for any  $i_0 \geq 0$ :

$$\frac{1}{m} \sum_{i=i_0+1}^{i_0+m} |\phi_i^T \tilde{\theta}|^2 \geq \alpha^2 \|\tilde{\theta}\|^2 > 0 \text{ and } \sum_{i=i_0+1}^{i_0+m} |\phi_i^T \hat{\theta}| > 0 \quad (36)$$

$\phi_i$  is deterministic for fixed  $\hat{\theta}$ , and  $\phi_i^T \tilde{\theta}$  is fixed and independent of  $w_i$ . Because the  $w_i$ 's are independent, the bound  $\epsilon$  is tight, i.e.  $w_i$  hits both the positive and negative bounds with a non-zero probability, the equation below follows for some  $p > 0$  independent of  $i_0$ .

$$\text{Prob}\left\{\epsilon^2 - \frac{1}{m} \sum_{i=i_0+1}^{i_0+m} w_i^2 \leq \frac{1}{m} \sum_{i=i_0+1}^{i_0+m} |\phi_i^T \tilde{\theta}|^2 \text{ and } \sum_{i=i_0+1}^{i_0+m} \phi_i^T \tilde{\theta} w_i > 0\right\} \geq p > 0 \quad (37)$$

Now,

$$\frac{1}{m} \sum_{i=i_0+1}^{i_0+m} |\phi_i^T \tilde{\theta}|^2 \geq \epsilon^2 - \frac{1}{m} \sum_{i=i_0+1}^{i_0+m} w_i^2 \quad \text{and} \quad \sum_{i=i_0+1}^{i_0+m} \phi_i^T \tilde{\theta} w_i > 0 \quad (38)$$

implies

$$\begin{aligned} \frac{1}{m} \sum_{i=i_0+1}^{i_0+m} |\phi_i^T \tilde{\theta}|^2 &\geq \epsilon^2 - \frac{1}{m} \sum_{i=i_0+1}^{i_0+m} w_i^2 \\ &> \epsilon^2 - \frac{1}{m} \sum_{i=i_0+1}^{i_0+m} w_i^2 - \frac{2}{m} \sum_{i=i_0+1}^{i_0+m} \phi_i^T \tilde{\theta} w_i \end{aligned} \quad (39)$$

and in turn

$$\begin{aligned} \frac{1}{m} \sum_{i=i_0+1}^{i_0+m} (y_i - \phi_i^T \hat{\theta})^2 &= \frac{1}{m} \sum_{i=i_0+1}^{i_0+m} (\phi_i^T \tilde{\theta} + w_i)^2 \\ &= \frac{1}{m} \sum_{i=i_0+1}^{i_0+m} |\phi_i^T \tilde{\theta}|^2 + \frac{1}{m} \sum_{i=i_0+1}^{i_0+m} w_i^2 + \frac{2}{m} \sum_{i=i_0+1}^{i_0+m} \phi_i^T \tilde{\theta} w_i > \epsilon^2. \end{aligned} \quad (40)$$

Thus,

$$\text{Prob}\left\{\frac{1}{m} \sum_{i=i_0+1}^{i_0+m} (y_i - \phi_i^T \hat{\theta})^2 > \epsilon^2\right\} \geq p \quad (41)$$

or

$$\text{Prob}\left\{\frac{1}{m} \sum_{i=i_0+1}^{i_0+m} (y_i - \phi_i^T \hat{\theta})^2 \leq \epsilon^2\right\} \leq (1 - p) \quad (42)$$

Therefore,

$$\begin{aligned} \text{Prob}\{z_k > \epsilon^2\} &= 1 - \text{Prob}\{z_k \leq \epsilon^2\} \\ &= 1 - \text{Prob}\left\{\frac{1}{m} \sum_{i=1}^m (y_i - \phi_i^T \hat{\theta})^2 \leq \epsilon^2\right\} \dots \\ &\text{Prob}\left\{\frac{1}{m} \sum_{i=(k-1)m+1}^{km} (y_i - \phi_i^T \hat{\theta})^2 \leq \epsilon^2\right\} \\ &\geq 1 - (1 - p)^k \rightarrow 1 \text{ as } k \rightarrow \infty \end{aligned} \quad (43)$$

The equations above show that  $\hat{\theta} = \theta$  is excluded from  $S_N^p(\epsilon)$  in probability which means that the diameter of  $S_N^p(\epsilon)$ ,  $\text{dia } S_N^p(\epsilon) \rightarrow 0$  in probability. If this was not true, then  $S_N^p(\epsilon)$  would contain points other than  $\theta$  for any  $N$  with non-zero probability, contradicting the fact that  $\hat{\theta} = \theta$  is excluded from  $S_N^p(\epsilon)$  in probability.  $\text{dia } S_N^p(\epsilon)$  converging to zero in probability means that at least one subsequence of  $S_N^p(\epsilon)$  converges to zero with probability 1. Because  $S_{k+1}^p(\epsilon) \subseteq S_k^p(\epsilon)$  implies that  $\text{dia } S_N^p(\epsilon)$  is nonincreasing, any subsequence of  $\text{dia } S_N^p(\epsilon)$  converging to zero with probability 1 implies that

dia  $S_N^p(\epsilon)$  converges to zero with probability 1 [9].

#### 4.3.1 Rate of Parameter Set Convergence

It has been shown that if the conditions in the previous section are met, the membership set diameter will converge to zero with probability 1. The rate of this convergence to zero, however, is highly dependent on the shape of the distribution of the disturbance, particularly at its bounds. If the distribution for the disturbance has a lot of mass at its end points, i.e. the probability that the disturbance lies on its bound is high, then the convergence rate will be fast. Likewise if the probability that the noise will hit the boundary is low, then the convergence rate is much slower [9].

## 5 Persistent Excitation

The importance of a persistently exciting regressor was discussed in the previous section along with how it relates to convergence of the parameter set. This section will discuss how the persistent excitation condition is formulated within the context of the formulation discussed in section 4.1.

The persistent excitation condition (34) can be written similarly as

$$n\alpha^2 I \succeq \sum_{k=t-n+1}^t D_k^T D_k \succeq n\beta^2 I, \quad (44)$$

for a suitable window length  $n$ , where  $D_k = D(x_k, u_k)$ , and  $D(x, u)$  is defined in equation 22. The difficulty with this condition lies with the fact that it is generally not convex in  $x$  and  $u$ , thus a convex sufficient condition must be derived to include this PE condition into the problem formulation in a relatively straightforward way.

### 5.1 Convex Sufficient Condition for Persistent Excitation

The derivation for a convex sufficient condition for persistent excitation begins by assuming a control input  $u_{0|t}^o$  that satisfies the state and input constraints has been obtained at time  $t$ . A perturbation  $\delta u$  is applied to  $u_{0|t}^o$  in an attempt to make the control input persistently exciting:

$$u_t = u_{0|t}^o + \delta u \quad (45)$$

Thus, the persistent excitation condition can be rewritten in the following manner.



$$\begin{aligned}
\sum_{k=t-n+1}^t D_k^T D_k &= \sum_{k=t-n+1}^{t-1} D_k^T D_k + D(x_t, u_t)^T D(x_t, u_t) \\
&= \sum_{k=t-n+1}^{t-1} D_k^T D_k + D(x_t, u_{0|t}^o + \delta u)^T D(x_t, u_{0|t}^o + \delta u),
\end{aligned} \tag{46}$$

but,

$$\begin{aligned}
D(x_t, u_{0|t}^o + \delta u) &= [A_1 x_t + B_1(u_{0|t}^o + \delta u) \ \dots \ A_p x_t + B_p(u_{0|t}^o + \delta u)] \\
&= [A_1 x_t + B_1 u_{0|t}^o \ \dots \ A_p x_t + B_p u_{0|t}^o] + [B_1 \delta u \ \dots \ B_p \delta u] \\
&= D(x_t, u_{0|t}^o) + L(\delta u) \quad \text{where } L(\delta u) = [B_1 \delta u \ \dots \ B_p \delta u].
\end{aligned} \tag{47}$$

Substituting back into equation 46:

$$\begin{aligned}
\sum_{k=t-n+1}^t D_k^T D_k &= \sum_{k=t-n+1}^{t-1} D_k^T D_k + (D(x_t, u_{0|t}^o) + L(\delta u))^T (D(x_t, u_{0|t}^o) + L(\delta u)) \\
&= \sum_{k=t-n+1}^{t-1} D_k^T D_k + D(x_t, u_{0|t}^o)^T D(x_t, u_{0|t}^o) + D(x_t, u_{0|t}^o)^T L(\delta u) \\
&\quad + L(\delta u)^T D(x_t, u_{0|t}^o) + L(\delta u)^T L(\delta u)
\end{aligned} \tag{48}$$

The persistent excitation condition can thus be reformulated as

$$\sum_{k=t-n+1}^t D_k^T D_k = M_t + D_t^T D_t = M_t + L(\delta u)^T D(x_t, u_{0|t}^o) + D(x_t, u_{0|t}^o)^T L(\delta u) + L(\delta u)^T L(\delta u) \succeq n\beta^2 I \tag{49}$$

where  $M_t$  is independent of  $\delta u$ ,

$$M_t = \sum_{k=t-n+1}^{t-1} D_k^T D_k + D(x_t, u_{0|t}^o)^T D(x_t, u_{0|t}^o) \tag{50}$$

and  $L(\delta u)$  is linear in  $\delta u$

$$L(\delta u) = [B_1 \delta u \ \dots \ B_p \delta u]. \tag{51}$$

The quadratic term  $L(\delta u)^T L(\delta u)$  is positive semi-definite so a sufficient condition for equation 44 to hold is

$$M_t + L(\delta u)^T D(x_t, u_{0|t}^o) + D(x_t, u_{0|t}^o)^T L(\delta u) \succeq n\beta_1^2 \mathbb{I}. \tag{52}$$

Equation 52 is a linear matrix inequality constraint on  $\delta u$  which is convex in  $\delta u$  and guarantees that the PE condition 44 is met with a degree of conservativeness based on  $\delta u$  as  $O(\|\delta u\|^2)$ .

The only decision variable in equation 52 is the disturbance on the input  $\delta u$  at the current time

step, so there is no guarantee that there will be a feasible solution for  $\delta u$  that satisfies the state and input constraints as well as equation 52. However, this may not necessarily cause a problem as the PE condition does not need to hold for every time step to still guarantee the convergence of the parameter set diameter to zero.

## 6 Implementation

This section initially discusses how the MPC algorithm is implemented in [1], and subsequently presents two new MPC algorithms. The first of these builds on the tube MPC of [1] using H-form polytopes in the tube description but employs a different cost. The second proposes a tube formulation in terms of both H- and V-form polytopes that allows a PE constraint to be applied to multi-step predictions rather than just a single predicted timestep (as in [1]).

H-form, short for half-space representation, of sets are the representation of sets in the manner that this report has considered until this point; an H-form set is defined as  $S = \{s : As \leq b\}$ . By Motzkin's theorem, for each H-form polytope, the convex hull of its vertices defines the same sets in the form of a V-polytope, and vice versa [11].

### 6.1 Existing MPC Algorithm [1]

In [1], Lu and Cannon combine the theory discussed in sections 3-5 to formulate an adaptive MPC algorithm with guarantees of recursive feasibility and stability. They make use of the algorithm described in section 3 along with a set based model identification technique for parameter estimation, and an implementation of the persistent excitation condition. Their proposed algorithm is as follows:

*Algorithm 1: Robust Adaptive MPC:*

**Offline**, for an initial parameter set estimate  $\Theta_0$ , choose  $V$  and compute the following values:

$K, \lambda$  from equation 19

$H_c, \hat{H}_1, \dots, \hat{H}_{n_\alpha}$  from equations 9 and 12

**Online** at time  $t \in \mathbb{N}_{\geq 0}$  given a state measurement  $x_t$ :

- 1) Update  $\Theta_t$  using the parameter set identification algorithm 24 and compute the vertices of  $\Theta_t$  as  $\theta_t^{(1)}, \dots, \theta_t^{(m)}$ .
- 2) Update  $\lambda_t$  by solving

$$\lambda_t = \max_{j,i} \hat{\theta}_t^{(j)T} \hat{H}_i \mathbf{1}. \quad (53)$$

3) Compute the optimal solution:  $\mathbf{v}_t, \boldsymbol{\alpha}_t$  of the LP

$$J^o(x_t) = \min_{\mathbf{v}, \boldsymbol{\alpha}} \sum_{k=0}^{N-1} J(x_t, u_t) \quad (54)$$

s.t. equations 8, 11, 16, 17, 18.

4) Calculate the control law  $u_{0|t}^o = Kx_t + v_{0|t}$  and check whether the PE condition 44 is satisfied with  $D_t = D(x_t, u_{0|t}^o)$ .

(a) If condition 44 is satisfied, implement  $u_t = u_{0|t}^o$

(b) Otherwise, recompute the optimization 54 with an additional optimization variable  $\delta u$  and with the convex PE condition 52 derived in the previous section.

(i) If the optimization is infeasible, implement  $u_t = u_{0|t}^o$ .

(ii) Otherwise implement  $u_t = u_{0|t}^o + \delta u$ .

The control input serves the dual purpose of stabilising the system and providing the requisite excitation so that the model parameters can be identified. These may at times be conflicting constraints on the control input. In cases where it is not possible to satisfy the system constraints and the PE constraints, the algorithm is designed for system constraint satisfaction to take precedence over satisfaction of the PE constraints [1].

This algorithm applied to a numerical example with a second-order discrete-time uncertain linear system highlights the advantages of the algorithm that Cannon and Lu have proposed. The specific numerical example that the algorithm is applied to is taken from a paper by Lorenzen et al. [10]. The model parameters are given by

$$\begin{aligned} A_0 &= \begin{bmatrix} 0.5 & 0.2 \\ -0.1 & 0.6 \end{bmatrix} & B_0 &= \begin{bmatrix} 0 \\ 0.5 \end{bmatrix} \\ A_1 &= \begin{bmatrix} 0.042 & 0 \\ 0.072 & 0.03 \end{bmatrix} & B_1 &= \begin{bmatrix} 0 \\ 0 \end{bmatrix} \\ A_2 &= \begin{bmatrix} 0.015 & 0.019 \\ 0.009 & 0.035 \end{bmatrix} & B_2 &= \begin{bmatrix} 0 \\ 0 \end{bmatrix} \\ A_3 &= \begin{bmatrix} 0 & 0 \\ -0 & 0 \end{bmatrix} & B_3 &= \begin{bmatrix} 0.0397 \\ 0.059 \end{bmatrix} \end{aligned} \quad (55)$$

and the true system parameter is  $\theta^* = [0.8 \ 0.2 \ -0.5]^T$ . The initial parameter set estimate is given by

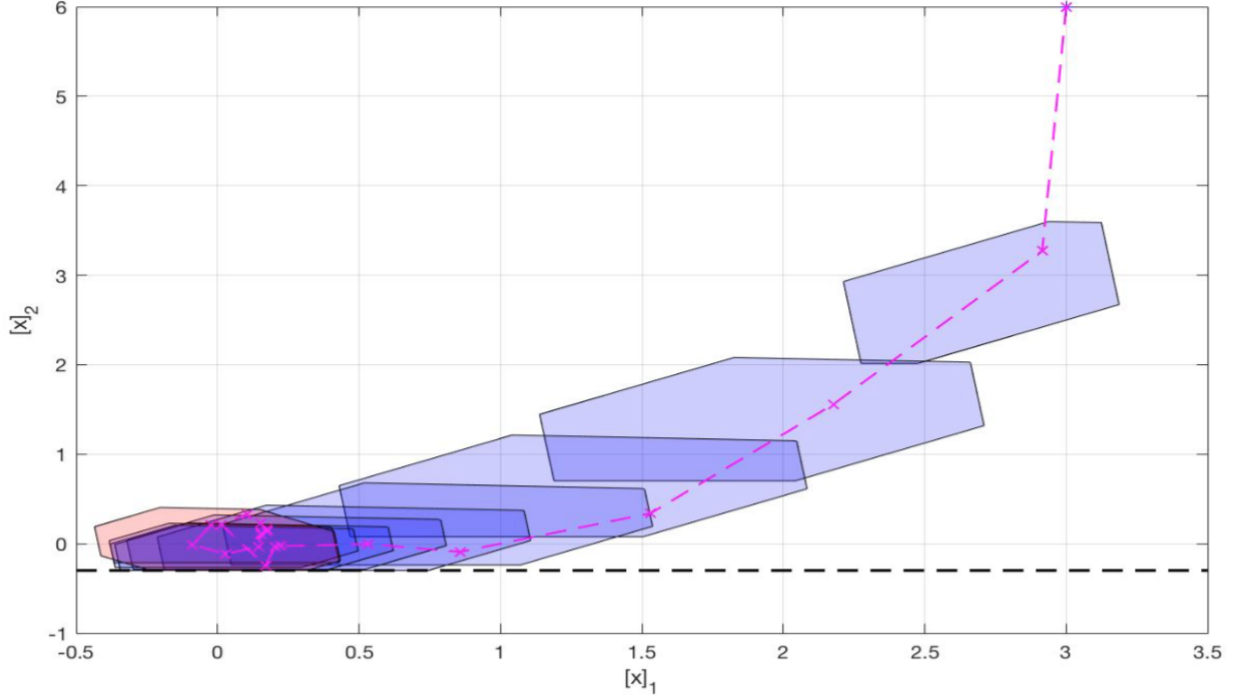


Figure 1: Closed loop state trajectory from initial condition  $x_0 = (3, 6)$ , and predicted state tube (polygons)  $\{\mathbb{X}_0, \dots, \mathbb{X}_N\}$  at time  $t = 0$  [1]

the hypercube centred on the origin with side length two ( $\Theta_0 = \{\theta : \|\theta\|_\infty \leq 1\}$ ) and the elements of the disturbance sequence are independently and identically distributed on  $\mathbb{W} = \{w \in \mathbb{R}^2 : \|w\|_\infty \leq 0.1\}$ . The state and input constraints are  $[x_t]_2 \geq -0.3$ , and  $u_t \leq 1$ .

The cross-sections of the robust state tubes predicted at time  $t = 0$  resulting from the robust adaptive MPC algorithm are shown below in Figure 1. The state constraint  $[x_t]_2 \geq -0.3$  is represented by the dashed black line in Figure 1 and it can be seen that the predicted state tubes never violate this constraint. This means that the state constraints are satisfied for all realisations of uncertainty and disturbance. Furthermore, it can be seen from the dashed pink line in the figure that the evolution of states converges to be in a neighbourhood close to 0, implying stability of the system.

It can be seen from examining plots of the parameter set over time that the proposed algorithm also leads to the convergence of the parameter set to a singleton at the true parameter value over the course of a sufficiently long period of time. Figure 2 shows that the reduction over time of the size of the parameter set is substantial. The volume of the parameter set is nearly quartered after the first time step, and the volume after the 10th time step is merely 13 percent of the original volume. After 5000 time steps, the volume of the parameter set is 0.0089 percent of the original volume, meaning nearly all of the model uncertainty has been eliminated. At this point, the parameter set is essentially a point at the true parameter value.

It is important to highlight that the decreasing uncertainty of the true parameter values leads

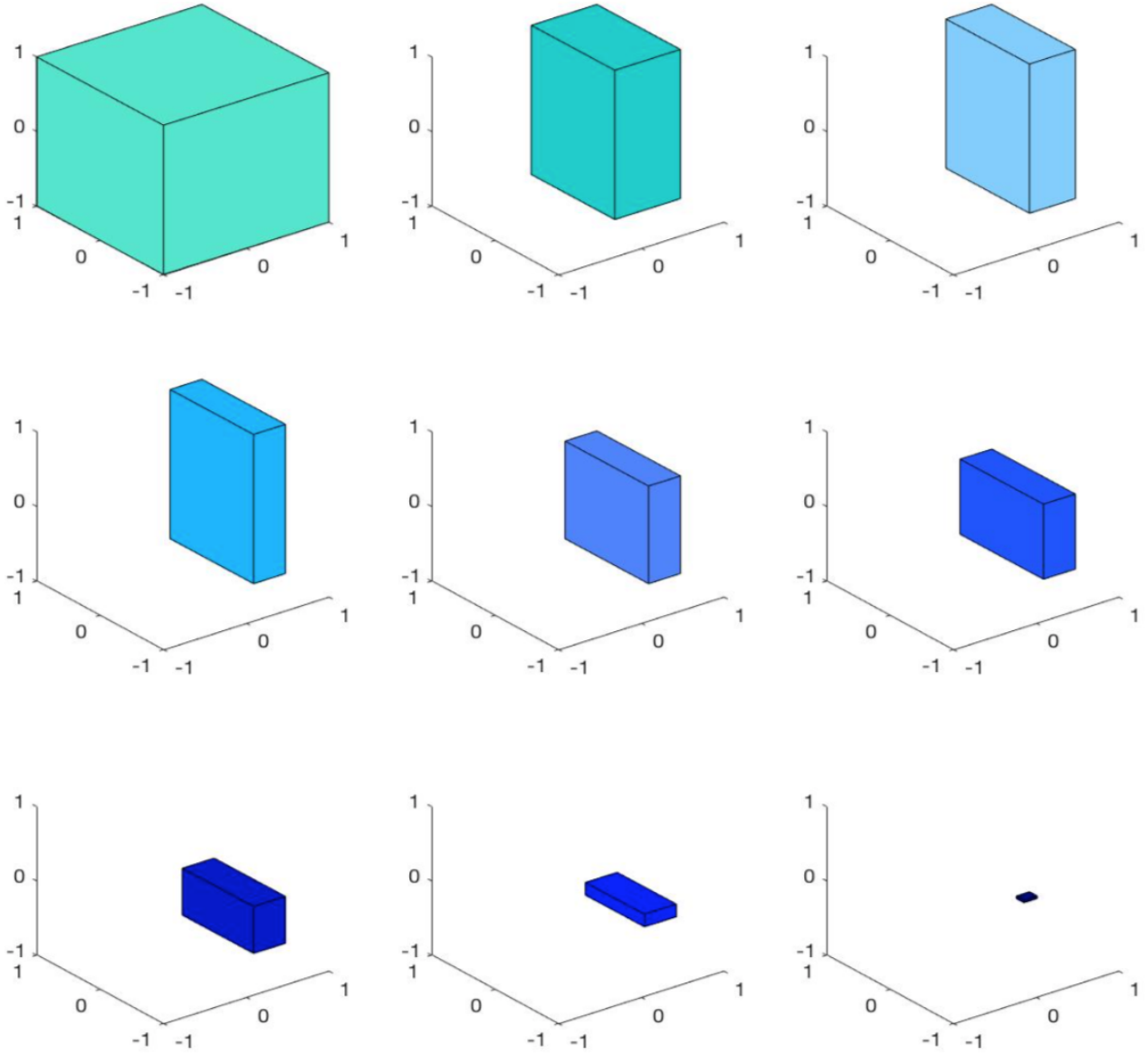


Figure 2: Parameter set  $\Theta_t$  at time steps  $t = 0, 1, 2$  (1st row)  $t = 10, 25, 50$  (2nd row) and  $t = 100, 500, 5000$  (3rd row) [1]

to a tangible improvement in performance; The decrease in size of  $\Theta_t$  leads directly to a decrease in the optimal value of the MPC cost for a given value of  $x_t$  and the same set of constraints. For the numerical example cited in Cannon and Lu's paper, the optimal predicted cost given the initial parameter set estimate  $\Theta_0$  gives  $J^o(x) = 62.2$  for  $x = x_0 = (3, 6)$ , while  $\Theta_{500}$  gives  $J^o(x) = 57.9$ , a 6.9% reduction versus the initial parameter set, and  $\Theta_{5000}$  gives  $J^o = 53.9$ , a 13.3% reduction. To compare, no parameter uncertainty gives a predicted optimal cost of  $J^o(x) = 52.70$ , which is a 15.3% reduction to the initial predicted optimal cost with the initial estimate for the parameter set. This report will also consider the performance of the proposed algorithm on the same numerical example to aid the understanding of the differing performance of the algorithm outline in previous section, and the new algorithm proposed by the author in the coming sections.

## 6.2 H-form Implementation

This section proposes a new MPC algorithm based on H-form polytopic tubes that follows closely from the theory set out in the previous sections and the proposed algorithm from above. An important deviation between the two implementations is the choice of objective function. Here, nominal cost function of the form

$$J(x_k, v_k) = \mathbf{v}_k^T H \mathbf{v}_k + 2\mathbf{f}^T \mathbf{v}_k \quad (56)$$

is proposed as opposed to an expected value cost  $J(x, u) = \sum_{i=0}^{\infty} \mathbb{E}(x_{i|k}^T Q x_{i|k} + u_{i|k}^T R u_{i|k})$  or a piecewise-linear worst case cost  $\max_{x_k \in \mathbb{X}, k=0,1,\dots} \sum_{k=0}^{\infty} (\max\{Qx_k\} + \max\{Ru_k\})$ . The cost is referred to as a nominal cost because  $H$  and  $f$  are chosen so that  $J$  represents a performance cost evaluated for predicted state and input sequences generated by a system model with a nominal parameter point estimate  $\hat{\theta}$ . Several factors contributed to the choice of a nominal quadratic cost as opposed to another cost function: firstly, the piecewise-linear min-max cost is very conservative when the parameter set is big (initially), whereas the nominal cost based on a point estimate is only as inaccurate as the point estimate itself. Furthermore, it is not straightforward to choose the weights of the min-max cost function, whereas it is simple to choose the weights of the quadratic nominal cost based on the theory of LQR controllers. Finally, the quadratic cost decouples the constraints from the cost calculation, which allows for more freedom in the way that the constraints are defined.

If the parameter vector  $\theta$  in (1) is equal to a given nominal parameter vector  $\hat{\theta}$ , then the dependence of the state predictions  $\mathbf{x}_k = (x_{0|k}, x_{1|k}, \dots, x_{N|k})$  on the predicted inputs  $\mathbf{u}_k = (u_{0|k}, u_{1|k}, \dots, u_{N|k})$  is linear. Thus the general quadratic predicted cost  $J(x_k, u_k) = \sum_{i=0}^N (\|x_{i|k}\|_Q^2 + \|u_{i|k}\|_R^2)$  can be represented as a quadratic function of the input sequence  $\mathbf{u}_k$  if  $\theta = \hat{\theta}$ . The cost can thus be represented as a function of  $\mathbf{u}$ :

$$J(x_k, u_k) = \mathbf{u}_k^T H \mathbf{u}_k + 2\mathbf{f}^T \mathbf{u}_k + g \quad (57)$$

$H$  is a constant positive (semi)definite matrix,  $\mathbf{f} = \mathbf{f}(x_k)$  is a vector depending on  $x_k$ , and  $g = g(x_k)$  is a scalar depending on  $x_k$ . The online optimisation thus becomes:

$$\begin{aligned} \min_{\mathbf{u}} \quad & \mathbf{u}^T H \mathbf{u} + 2\mathbf{f}^T \mathbf{u} \\ \text{subject to} \quad & \end{aligned} \quad (58)$$

It is easy to show that this problem is a convex optimisation problem so long as the constraints are convex due to the restriction that  $H$  is a positive (semi)definite matrix.

The general quadratic cost over an infinite horizon  $J(x_k, \mathbf{u}_k) = \sum_{i=0}^{N-1} (\|x_{i|k}\|_Q^2 + \|u_{i|k}\|_R^2) + \|x_{N|k}\|_Q^2$  can be written in the form of equation 57. To do so, begin by writing the predicted states in terms of

the current state and predicted inputs:

$$\begin{aligned}
x_{0|k} &= x_k \\
x_{1|k} &= Ax_k + Bu_{0|k} \\
x_{2|k} &= A^2x_k + ABu_{0|k} + Bu(k+1|k) \\
&\vdots \\
x_{N|k} &= A^Nx_k + A^{N-1}Bu_{0|k} + A^{N-2}Bu(k+1|k) + \dots + Bu(k+N-1|k)
\end{aligned} \tag{59}$$

This can be written in a compact way

$$\begin{aligned}
x_{i|k} &= A^i x_k + C_i \mathbf{u}_k, \quad i = 0, \dots, N \\
\text{or } \mathbf{x}_k &= Mx_k + C\mathbf{u}_k, \quad \text{where } M = \begin{bmatrix} A \\ A^2 \\ \vdots \\ A^N \end{bmatrix}.
\end{aligned} \tag{60}$$

Consequently, the  $C$  matrix is defined by

$$\begin{bmatrix} B & 0 & \dots & 0 \\ AB & B & \dots & 0 \\ \vdots & \vdots & \ddots & \vdots \\ A^{N-1}B & A^{N-2}B & \dots & B \end{bmatrix} \tag{61}$$

In the sections above, the optimal control input  $u_{0|k}$  has been defined by  $u_{0|k} = Kx_k + v_{0|k}$ , so the above equations can be rewritten as

$$\begin{aligned}
x_{i|k} &= \Phi^i x_k + C_i \mathbf{v}_k, \quad i = 0, \dots, N \\
\text{or } \mathbf{x}_k &= Mx_k + C\mathbf{v}_k, \quad \text{where } M = \begin{bmatrix} \Phi \\ \Phi^2 \\ \vdots \\ \Phi^N \end{bmatrix},
\end{aligned} \tag{62}$$

where  $\Phi$  is defined as  $\Phi = A + BK$ , and the  $C$  matrix is defined in the same way as above, but  $A$  is replaced with  $\Phi$ . Substituting for  $x_{i|k}$  into equation 57 yields:

$$J_k = x_k^T M^T \bar{Q} M x_k + 2x_k^T M^T \bar{Q} C \mathbf{v}_k + \mathbf{v}_k^T (C^T \bar{Q} C + \bar{R}) \mathbf{v}_k \tag{63}$$

where,

$$\bar{Q} = \begin{bmatrix} Q & 0 & \dots & 0 \\ 0 & \ddots & & \vdots \\ \vdots & & Q & 0 \\ 0 & \dots & 0 & P \end{bmatrix} \quad (64)$$

$$\bar{R} = \begin{bmatrix} R & & \\ & \ddots & \\ & & R \end{bmatrix}$$

and  $P$  is the solution to the Lyapunov equation  $P - (A + BK)^T P (A + BK) = Q + K^T R K$ . For the numerical example considered in this report,  $Q$  was taken to be an identity matrix of size two, and  $R = 1$ . Equation (63) can be rewritten as  $J(x_k, u_k) = x_k^T M^T \bar{Q} M x_k + 2 \mathbf{f}^T \mathbf{v}_k + \mathbf{v}_k^T H \mathbf{v}_k$  where  $H = C^T \bar{Q} C + \bar{R}$  and  $\mathbf{f}^T = x_k^T M^T \bar{Q} C$ . The first term is a constant, and thus for the purposes of the online optimisation, the cost function can be rewritten as  $J(x_k, u_k) = 2 \mathbf{f}^T \mathbf{v}_k + \mathbf{v}_k^T H \mathbf{v}_k$  which is identical to the form in equation 56 that was stated in the beginning of this section [3].

The H-form adaptive MPC algorithm proposed in this report is detailed below:

**Offline:**

- 1) Set the number of time steps the simulation will run for
- 2) Set prediction horizon
- 3) Define system matrices
- 4) Define set that the disturbance lies in, and define initial parameter set estimate  $\Theta_0$
- 5) Define initial condition and true model parameter value
- 6) Define matrices  $F$  and  $G$  that formulate state and input constraints
- 7) Generate  $V$  matrix and calculate stabilising gain  $K$  from  $V$
- 8) Calculate  $H_c$  and  $\hat{H}_i$  from the LPs in equations 9 and 12 respectively
- 9) Define  $Q$  and  $R$  for use in constructing the cost function
- 10) Compute  $\mu$  for use in calculating point estimates of the model parameters

**Online:**

- 1) Do parameter set update
- 2) Compute vertices of new parameter set
- 3) Compute radial size of the new parameter set
- 4) Calculate a point estimate according to equation 25
- 5) Optimise the cost function to compute the optimal control input for next time step



- a) Formulate cost function in terms of cost matrices
- b) Set constraints according to equation 54
- c) Optimise cost function and return optimal control input
- 6) Simulate the evolution of the system to its next state given the calculated control input
- 7) Repeat until previously specified number of time steps has been simulated

The prediction horizon was set to 10 time steps, and the system matrices are as defined in equation (55). The initial parameter set was defined to be a hypercube centred on the origin with side length two. The complexity of the parameter set was restricted to be a hypercube so that the calculation of the parameter sets vertices would be straightforward and computationally light. The parameter set is defined as  $\Theta_k = \{\theta : [I \quad -I]^T \theta \leq \pi_{\theta,k}\}$ . Note that computing the vertices of a hypercube with given side lengths, centred on the origin is trivial; the method used here for calculating the vertices of the parameter set first translates the parameter set so that it is centred on the origin, computes the vertices (trivially), then translates these vertices to be centred on the centre of the parameter set. To do this,  $\pi_{\theta,k}$  is represented as  $[\bar{\pi} \quad \underline{\pi}]^T$ . The centre of the parameter set  $\theta_0$  is defined as  $\frac{1}{2}(\bar{\pi} - \underline{\pi})$ . The parameter set, shifted to be centred on the origin, is now defined as

$$\Theta_c = \left\{ \theta : \begin{bmatrix} I \\ -I \end{bmatrix} (\theta - \theta_0) \leq \begin{bmatrix} \bar{\pi} - \theta_0 \\ \underline{\pi} + \theta_0 \end{bmatrix} \right\}. \quad (65)$$

Substituting the value for  $\theta_0$  in equation 65 results in

$$\Theta_c = \left\{ \theta : \begin{bmatrix} I \\ -I \end{bmatrix} (\theta - \theta_0) \leq \begin{bmatrix} \frac{1}{2}(\bar{\pi} + \underline{\pi}) \\ \frac{1}{2}(\bar{\pi} + \underline{\pi}) \end{bmatrix} \right\}, \quad (66)$$

which is of the form

$$\Theta = \left\{ \theta : \begin{bmatrix} I \\ -I \end{bmatrix} (\theta - \theta_0) \leq \begin{bmatrix} \pi \\ \pi \end{bmatrix} \right\}, \quad (67)$$

meaning that the set is now centred on the origin. The vertices of a set that has the form of equation (67) are found by performing an element-wise multiplication of  $\pi$  with each column of the matrix  $Z$  defined below

$$Z = \begin{bmatrix} 1 & 1 & 1 & 1 & -1 & -1 & -1 & -1 \\ 1 & 1 & -1 & -1 & 1 & 1 & -1 & -1 \\ 1 & -1 & 1 & -1 & 1 & -1 & 1 & -1 \end{bmatrix}. \quad (68)$$

The columns of  $Z$  give all the possible positive and negative permutations of the elements of  $\pi$  which corresponds to the vertices of the set. Having found the vertices of the centred parameter set, the

coordinates of the centre are added to each vertex, resulting in the vertices of the original parameter set. Computation of the diameter of the parameter set is done in a similar way. Bai et al. define the diameter of the membership set in (31). This is equivalent to the following optimisation

$$\rho(\Theta_k) = \max_i |\bar{\pi}_i - \underline{\pi}_i| \quad (69)$$

where  $\bar{\pi}$  and  $\underline{\pi}$  have the same meaning as in the equations above.

Numerical Simulations of this algorithm applied to the problem described in Section 6.1 produce results similar to those discussed in section 5.2. Figure 3 shows the state evolution of the system over thirty time steps using the algorithm proposed in this section. As can be seen from the figure, the

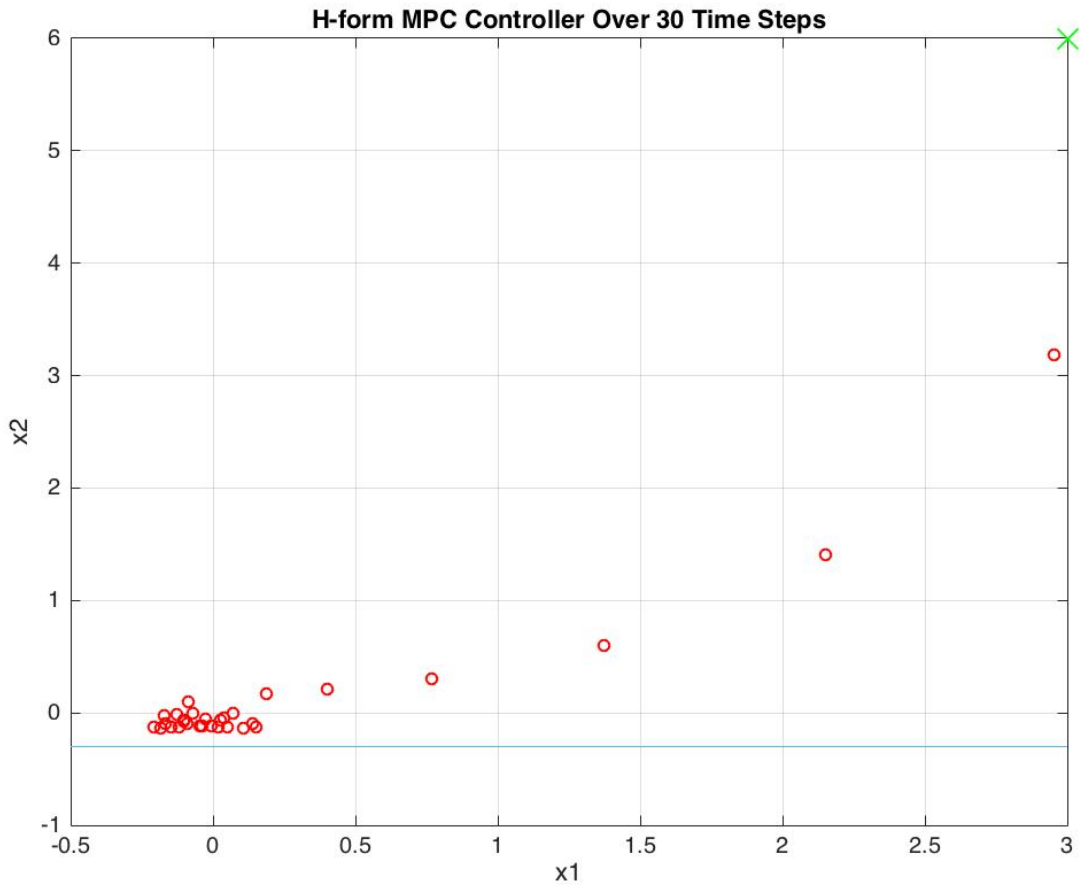


Figure 3: Evolution of system state over 30 time steps. Convergence of the system to a region around the origin can clearly be seen

states converge to a region around the origin quickly and never violate the state constraint that is plotted in light blue.

### 6.3 V-form Implementation

This section proposes a robust tube MPC formulation that allows a computationally tractable conversion between H-form representation and V-form representation of the state tube. An advantage of the V-form implementation is that the computation of the V-form of the parameter set estimate  $\Theta_k$  is no longer necessary. In the implementations of section 6.1 and section 6.2, the parameter set estimate was constrained to be a hypercube so that the computation required to calculate the vertices of the parameter set was simple. However, as the vertices of the parameter set are no longer needed, the shape of the parameter set need not be constrained to be in such a simple form, meaning that more accurate estimations for the parameter set can be achieved.

Another motivation for a tractable V-form implementation is the ease of implementation of the persistent excitation condition, which will be discussed later in this section.

The H-form algorithm discussed in the previous sections lends itself well to being converted to a V-form representation. To do so, the constraints must be formulated in terms of the vertices of the predicted state tube cross sections.

If  $\mathbb{X}_{i|k} \subset \mathbb{R}^n$  is used to denote a compact polytope defining the  $i$  steps ahead cross section of the predicted state tube at time  $k$ ,

$$\mathbb{X}_{i|k} = \{x : Vx \leq \alpha_{i|k}\}, \quad (70)$$

then  $\mathbb{X}_{i|k}$  can be represented equivalently with the vertex representation as the convex hull of the vertices of the cross section of the predicted state tube:

$$\mathbb{X}_{i|k} = \text{Co}\{x_{i|k}^j, j = 1, \dots, m\} \quad (71)$$

$x_{i|k}^j$  represents a single vertex of the cross section of the predicted state tube. The equivalency of the above representations is straightforward conceptually. In equation 70, the predicted state tube is represented as the space enclosed by the intersection of a set of half-spaces, where as equation 71 represents the same space as the convex hull of the vertices of the space. Let  $e_r$  be the  $r$ th column of the identity matrix in  $\mathbb{R}^{n_\alpha \times n_\alpha}$  where  $n_\alpha$  is the number of rows of the  $V$  matrix from previous sections. For each vertex of  $\mathbb{X}_{i|k}$  (for each  $j \in \{1, \dots, m\}$ ), the  $r$ th row of  $V$ ,  $e_r^T V$  and the  $r$ th element of  $\alpha_{i|k}$ ,  $e_r^T \alpha_{i|k}$  satisfy

$$e_r^T V x_{i|k}^j = e_r^T \alpha_{i|k} \quad \forall r \in \mathcal{R}_j \quad (72)$$

for some index set  $\mathcal{R}_j$  with  $|\mathcal{R}_j| = n$ . Importantly,  $\mathcal{R}_j$  can be computed offline as it is independent of  $\alpha_{i|k}$ . This is true because the allowable values of  $\alpha_{i|k}$  are such that each hyperplane in the H-form of

$\mathbb{X}_{i|k}$ , i.e. the hyperplanes described by each row of  $V$ , has a non-empty intersection with the boundary of  $\mathbb{X}_{i|k}$ . Thus, for each  $j \in \{1, \dots, m\}$  the following relation holds.

$$x_{i|k}^j = U^j \alpha_{i|k} \quad (73)$$

$U^j$  is a matrix of size  $n \times n_\alpha$  and is computed offline given knowledge of  $\mathcal{R}_j$ . The results stated above can be used to derive equivalent formulations of the H-form constraints in the online optimisation.

The constraint

$$Fx + G(Kx + v_{i|k}) \leq \mathbf{1} \quad \forall x \in \mathbb{X}_{i|k} \quad (74)$$

can be expressed equivalently in terms of the variables  $\alpha_{i|k}$  and  $v_{i|k}$  by the following expression:

$$(F + GK)U^j \alpha_{i|k} + Gv_{i|k} \leq \mathbf{1} \quad \forall j \quad (75)$$

The constraint

$$(A(\theta) + B(\theta)K)x + B(\theta)v_{i|k} + w \in \mathbb{X}_{i+1|k} \quad \forall w \in \mathcal{W}, \quad \forall x \in \mathbb{X}_{i|k}, \quad \forall \theta \in \Theta = \{\theta : H_\theta \theta \leq h_\theta\} \quad (76)$$

can be expressed equivalently as

$$V((A(\theta) + B(\theta)K)U^j \alpha_{i|k} + B(\theta)v_{i|k}) + \bar{w} \leq \alpha_{i+1|k} \quad \forall \theta \in \Theta, \quad \forall j \quad (77)$$

where  $e_l^T \bar{w} = \max_{w \in \mathcal{W}} e_l^T Vw$  for  $l = 1, \dots, n_\alpha$  and hence as

$$VD(U^j \alpha_{i|k}, KU^j \alpha_{i|k} + v_{i|k})\theta + Vd(U^j \alpha_{i|k}, KU^j \alpha_{i|k} + v_{i|k}) + \bar{w} \leq \alpha_{i+1|k} \quad \forall \theta \in \Theta, \quad \forall j \quad (78)$$

where  $A(\theta)x + B(\theta)u = D(x, u)\theta + d(x, u)$  ( $D(x, u)$  and  $d(x, u)$  are both linear functions in  $x$  and  $u$ ).

Finally, this is implemented in the online optimisation as the set of following constraints,

$$\begin{aligned} \Lambda_{i|k}^j H_\theta &= VD(U^j \alpha_{i|k}, KU^j \alpha_{i|k} + v_{i|k}) \\ \Lambda_{i|k}^j h_\theta &\leq \alpha_{i+1|k} - VD(U^j \alpha_{i|k}, KU^j \alpha_{i|k} + v_{i|k}) - \bar{w} \\ \Lambda_{i|k}^j &\geq 0 \end{aligned} \quad (79)$$

for  $i = 1, \dots, N - 1$  and  $j = 1, \dots, m$  where  $N$  is the prediction horizon length and  $m$  is the number of vertices of the cross section of the predicted state tubes. The constraints in equation 79 apply over the length of the prediction horizon; a version of these constraints that form the terminal constraints

must also be applied to the online optimisation so that it has an equivalent form to that of the H-form optimisation.

$$\begin{aligned}
\Lambda_{N|k}^j H_\theta &= VD(U^j \alpha_{N|k}, KU^j \alpha_{N|k}) \\
\Lambda_{N|k}^j h_\theta &\leq \alpha_{N|k} - Vd(U^j \alpha_{N|k}, KU^j \alpha_{N|k+}) - \bar{w} \\
\Lambda_{N|k}^j &\geq 0
\end{aligned} \tag{80}$$

To implement the V-form algorithm, the constraints from the H-form algorithm in the online optimisation are replaced by the constraints in (75), (79), and (80).

Having replaced the relevant H-form constraints with their V-form counterparts, the implementation of the proposed V-form algorithm is similar to the H-form algorithm. The algorithm is detailed below:

**Offline:**

- 1) Set the number of time steps the simulation will run for
- 2) Set prediction horizon
- 3) Define system matrices
- 4) Define set  $\mathbb{W}$  that the disturbance lies in, and define initial parameter set estimate  $\Theta_0$
- 5) Define initial condition and true model parameter value
- 6) Define matrices  $F$  and  $G$  that formulate state and input constraints
- 7) Generate  $V$  matrix and compute redundant rows of  $V$  and remove them
- 8) Compute stabilising gain  $K$  from  $V$  matrix
- 9) Define  $Q$  and  $R$  for use in constructing the cost function
- 10) Compute  $\mu$  for use in calculating point estimates of the model parameters

**Online:**

- 1) Do parameter set update
- 2) Compute radial size of the new parameter set
- 3) Calculate a point estimate according to equation 25
- 4) Optimise the cost function to compute the optimal control input for next time step
  - a) Construct cost matrices
  - b) Formulate cost function in terms of cost matrices
  - c) Set constraints according to equations 75, 79, and 80
  - d) Add additional constraint for current time step PE condition
  - e) Optimise cost function and return optimal control input
- 5) Simulate the evolution of the system to its next state given the calculated control input

6) Repeat until previously specified number of time steps has been simulated

In V-form, implementing the PE condition is simply a matter of including an extra constraint in the online optimisation of the form

$$M_0 + D(x_t, u_{0|t}^*)^T D(x_t, u_{0|t}^*) + D(x_t, u_{0|t}^*)^T \begin{bmatrix} B_1 \delta u & \dots & B_v \delta u \end{bmatrix} + \begin{bmatrix} B_1 \delta u \\ \vdots \\ B_v \delta u \end{bmatrix} D(x_t, u_{0|t}^*) \succeq \beta^2 I, \quad (81)$$

where

$$M_0 = \sum_{k=t-n+1}^{t-1} D(x_k, u_k)^T D(x_k, u_k) + D(x_t, u_{0|t}^o)^T D(x_t, u_{0|t}^o), \quad (82)$$

and the actual control input that is used for the system is given by

$$u_{0|k} = u_{0|k}^* + \delta u. \quad (83)$$

The cost function chosen in this algorithm is the same as in the H-form algorithm plus another term  $-\lambda\beta^2$ , so that the total cost function is given by

$$J(x_k, u_k) = 2f^T v_k + v_k^T H v_k - \lambda\beta^2 \quad (84)$$

and the matrices defining the cost are computed in the same way. The weighting  $\lambda$  in the second term gives the user a way to denote the relative importance that the controller places on stabilising the system versus having a high degree of persistent excitation. Not surprisingly, this version of the adaptive MPC algorithm has performance that is comparable with the H-form algorithm, however with slightly faster parameter set convergence due to the inclusion of the persistent excitation condition in this implementations. Figure 4 shows the evolution of the states with the V-form algorithm controller. As was the case in the H-form controller, it can be seen that the system quickly converges to a small region around the origin, and that the state constraints are satisfied for all time steps. Although the control inputs are not plotted on the graph, they also satisfy the input constraints of the system at all time steps.

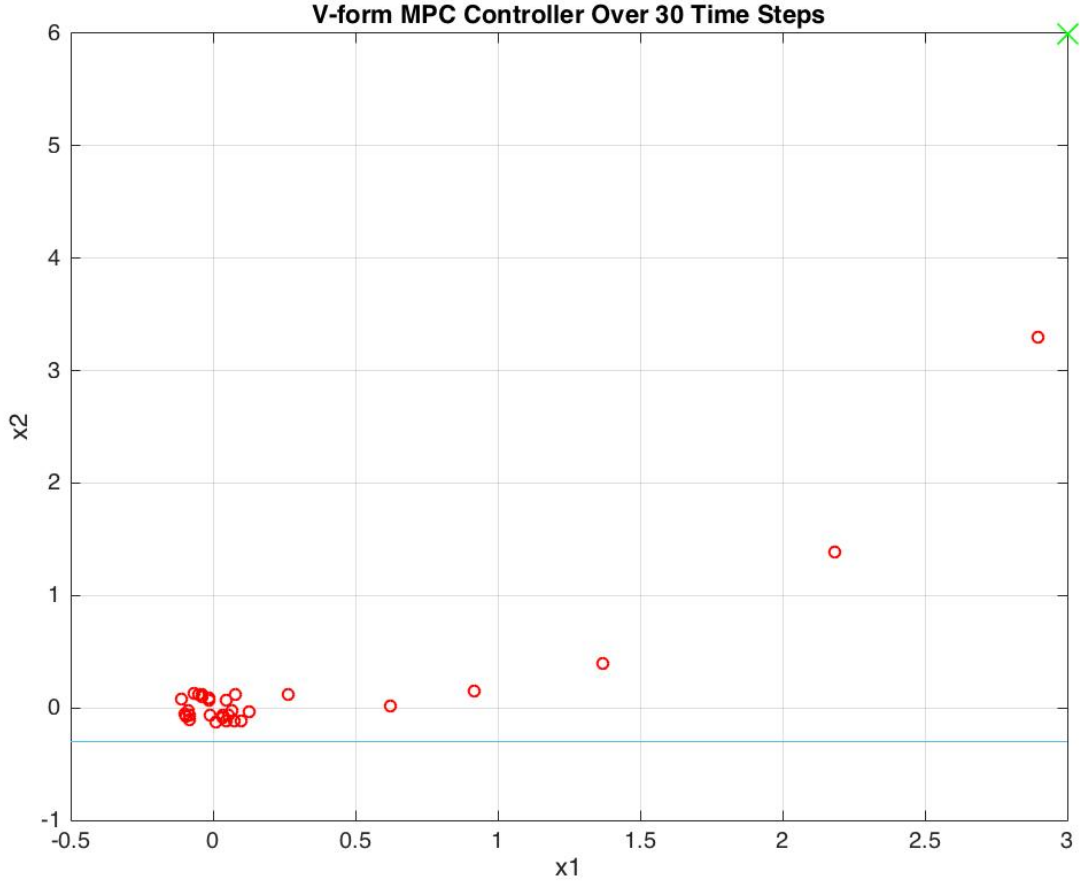


Figure 4: Evolution of system state over 30 time steps. Again, convergence to a region around the origin is clearly displayed

### 6.3.1 Calculation of $\mathcal{R}_j$ and $U^j$

Allowing  $\mathbb{X}(\alpha)$  to denote the subset of  $\mathbb{R}^n$  defined by

$$\mathbb{X}(\alpha) = \{x : Vx \leq \alpha\} \quad (85)$$

for  $\alpha \in \mathbb{R}^{n_\alpha}$  and  $V \in \mathbb{R}^{n_\alpha \times n_x}$ , let the vertices of  $\mathbb{X}(\alpha)$  be denoted by  $x^j(\alpha)$  for  $j = 1, \dots, m$  such that

$$\mathbb{X}(\alpha) = \text{Co}\{x^j(\alpha), j = 1, \dots, m\}. \quad (86)$$

Using this notation,  $\mathbb{X}_{i|k}$  will denote  $\mathbb{X}(\alpha_{i|k})$  and  $x_{i|k}^j = x^j(\alpha_{i|k})$ .

Assume that for a given vector  $\alpha$  (e.g vector of all ones), the polytope  $\mathbb{X}(\alpha)$  has the property that for each row of  $V$ , the hyperplane described by  $\{x : e_r^T Vx = e_r^T \alpha\}$  is a non-redundant face of  $\mathbb{X}(\alpha)$ , meaning that it intersects the boundary of  $\mathbb{X}(\alpha)$  at more than a single point ( $e_r^T$  represents the  $r$ th column of the identity matrix in  $\mathbb{R}^{n_\alpha \times n_\alpha}$ ). From simple geometric arguments and linear programming

duality, the conditions below provide a method of checking whether this property is satisfied, and of using it to compute  $\mathcal{R}_j$  and  $U^j$ .

**The following conditions are equivalent:**

- (a). For each  $r = 1, \dots, n_\alpha$ , the intersection of the hyperplane  $H_r(\alpha) = \{x : e_r^T V x = e_r^T \alpha\}$  with  $\mathbb{X}(\alpha)$  is non-empty and consists of more than a single point
- (b). For each  $r = 1, \dots, n_\alpha$ ,  $\mathbb{X}(\alpha) \subset \mathbb{X}(\alpha + e_r \epsilon)$  for all  $\epsilon > 0$ .
- (c). Each vertex  $x^j(\alpha)$  lies at the intersection of exactly  $n$  hyperplanes:  $H_{r_1^j}(\alpha) \cap H_{r_2^j}(\alpha) \cap \dots \cap H_{r_n^j}(\alpha) = \{x^j(\alpha)\}$  for some pairwise distinct set of indices  $R_j = \{r_1^j, \dots, r_n^j\} \subset \{1, \dots, n_\alpha\}$ .

By the equivalence of conditions (a) and (b), one can check whether condition (a) is satisfied by solving the linear programs in equation 87 for  $r = 1, \dots, n_\alpha$ . Condition (b) holds if and only if  $\bar{\alpha}_r > e_r^T \alpha$  for all  $r = 1, \dots, n_\alpha$ . It will always be the case that the allowable values for  $\alpha_{i|k}$  are such that each hyperplane in the description of  $\mathbb{X}_{i|k}$  has a non-empty intersection with the boundary of  $\mathbb{X}_{i|k}$  because otherwise  $\alpha_{i|k}$  would be a suboptimal solution of the online MPC optimisation. In implementing the linear program,

$$\begin{aligned} \bar{\alpha}_r = \max_x e_r^T V x \\ \text{subject to} \quad \begin{bmatrix} e_1^T \\ \vdots \\ e_{r-1}^T \\ e_{r+1}^T \\ \vdots \\ e_{n_\alpha}^T \end{bmatrix} V x \leq \begin{bmatrix} e_1^T \\ \vdots \\ e_{r-1}^T \\ e_{r+1}^T \\ \vdots \\ e_{n_\alpha}^T \end{bmatrix} \alpha \end{aligned} \quad (87)$$

it was found that  $\mathbb{X}(\alpha)$  had fewer facets than the number of rows of  $V$  (i.e.  $\bar{\alpha}_r \not> e_r^T \alpha$  for all  $r$ ) for the default value of  $\alpha$  (the value of  $\alpha$  for which  $\mathbb{X}(\alpha)$  was defined to be lambda-contractive), meaning that some rows of  $V$  were redundant. The redundant rows of  $V$  were the rows  $r$  that did not satisfy  $\bar{\alpha}_r > \alpha_r$ , where  $\bar{\alpha}$  calculated for each  $r$  by solving the linear program (87). Thus, one is able to remove the redundant rows of  $V$  without affecting  $\mathbb{X}(\alpha)$ , which has the benefits of satisfying the three conditions above and reducing the computation required in the online MPC optimisation without affecting the performance or feasibility properties of the MPC algorithm.

If condition (a) holds, and if the vertices  $x^j(\alpha)$  are known, then  $\mathcal{R}_j$  and  $U^j$  can be determined for each  $j = 1, \dots, m$  using condition (c). As a result,  $\mathcal{R}_j$  is the index set

$$\mathcal{R}_j = \{r \in \{1, \dots, m\} : e_r^T V x^j(\alpha) = e_r^T \alpha\} \quad (88)$$



and, having determined  $\mathcal{R}_j = \{r_1^j, \dots, r_n^j\}$ , we can determine  $U^j$  from the following relations:

$$\begin{bmatrix} e_{r_1^j}^T \\ \vdots \\ e_{r_n^j}^T \end{bmatrix} V x^j(\alpha) = \begin{bmatrix} e_{r_1^j}^T \\ \vdots \\ e_{r_n^j}^T \end{bmatrix} \alpha \Rightarrow U^j = \left( \begin{bmatrix} e_{r_1^j}^T \\ \vdots \\ e_{r_n^j}^T \end{bmatrix} V \right)^{-1} \begin{bmatrix} e_{r_1^j}^T \\ \vdots \\ e_{r_n^j}^T \end{bmatrix} \quad (89)$$

It is important to note that the matrix inverse term in the expression given for  $U^j$  in equation 89 necessarily has an inverse if condition (c) holds, which necessarily holds if condition (a) or (b) holds, and this can be enforced through removing the redundant rows of the  $V$  matrix.

## 6.4 Comparing H-Form and V-Form Implementations

As mentioned earlier, the performance of the H-form and V-form controllers are comparable. Figures 3 and 4 show that the system state converges to a region around the origin in a comparable fashion, and in both controllers the state and control inputs are satisfied for all time steps (and also all predicted time steps). The V-form controller shows slightly quicker convergence of the parameter set, but this is expected because of the implementation of the persistent excitation condition in the V-form controller but not in the H-form controller. Thus, this difference in convergence rate can be explained by the inclusion of the PE condition in the V-form controller, rather than an inherent property of the V-form implementation itself. Figure 5 shows the evolution of the parameter set diameter with each time step for the H-form implementation, and V-form implementation, respectively. As can be seen from the two figures, the final parameter set diameter after 100 time steps is slightly smaller for the V-form implementation compared to the H-form (approximately 0.2 vs approximately 0.3) due to the inclusion of the persistent excitation condition. As the figures show, the parameter set diameter is always non-increasing, but its behaviour is stochastic (the diameter decreases at random times by random amounts), making it very difficult to predict how long it will take for the parameter set estimate to converge to any specified neighbourhood of the true parameter value. It should be noted that the plots of parameter set diameter should not be compared to those in Cannon and Lu's paper [1] as the distribution used for the disturbance differs. Cannon and Lu use a uniformly distributed disturbance, while here the disturbance is projected onto the boundary of the disturbance set at each time step in order to reduce the simulation time required to observe convergence of the parameter set. All of the examples and implementations from this point on will consider disturbances that lie on the boundary of the disturbance set.

A good way to measure the performance of the two controllers is to examine the plots of the running sum of the squared states versus time. This plot gives insight into how well the controller is

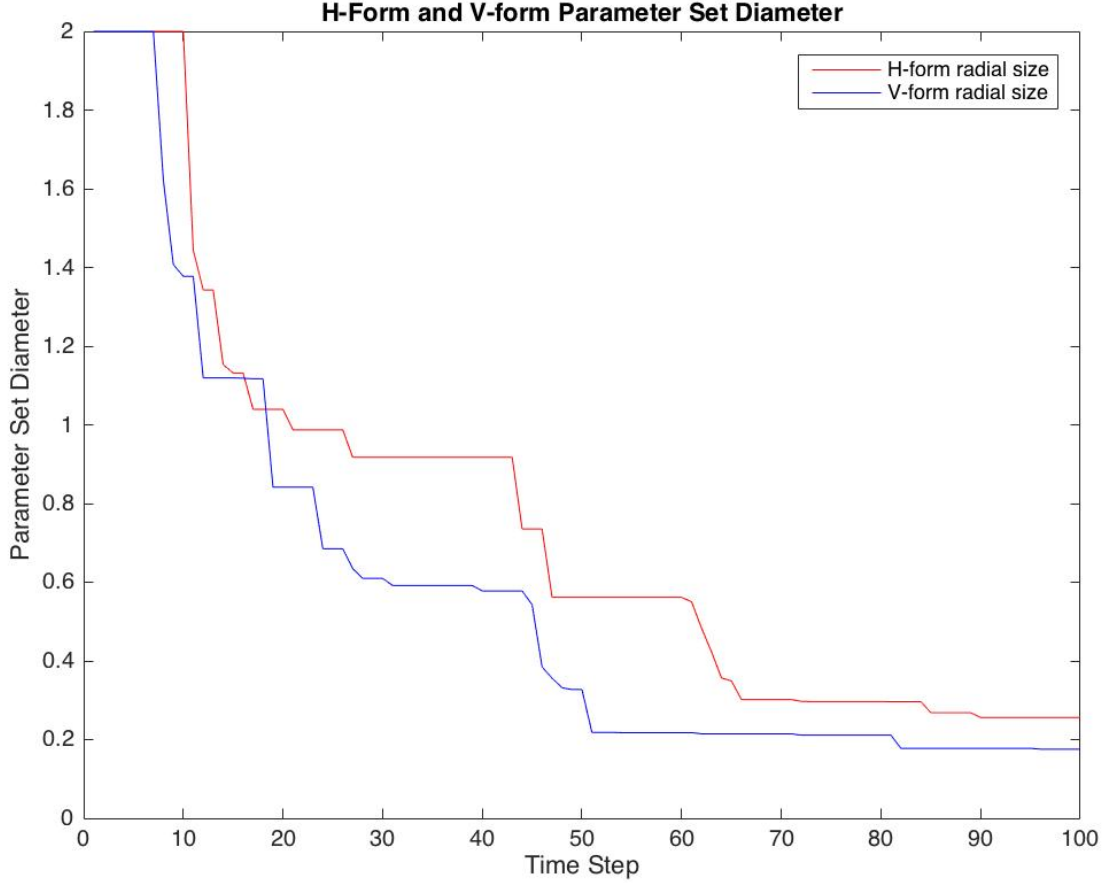


Figure 5: Evolution of parameter set diameter: H-form and V-form. The V-form controller shows faster convergence of the parameter set compared to H-form, which is down to inclusion of persistent excitation condition in V-form controller. Stochastic behaviour of the parameter set diameter is also evidenced.

performing, and after an initial section of high increase, the plot will level off and the average rate of increase of this sum will converge to a value proportional to the time-average of  $\|w_k\|^2$  since this is consistent with the mean square stability bound (90). This follows from the fact that the closed loop system with MPC control law  $u(x_k) = Kx_k + v_{0|k}^*$  is finite gain  $l_2$  stable (see e.g. [4], Theorem 14) meaning that there exists constants  $c_0, c_1, c_2 \in \mathbb{R}_{>0}$  such that for all  $K \in \mathbb{N}$

$$\sum_{k=0}^K \|x_k\|^2 \leq c_0 \|x_0\|^2 + c_1 \|\hat{\theta}_0 - \theta^*\|^2 + c_2 \sum_{k=0}^K \|w_k\|^2 \quad [4]. \quad (90)$$

Multiplying both sides of the inequality in (90) by  $(1/K)$  and considering the limit as  $K$  tends to infinity, the first two terms on the right hand side tend to zero, resulting in an inequality relating the mean square norm of  $x$  to the mean square norm of  $w$ . The sum of the magnitude of the states is bounded by the term  $c_0 \|x_0\|^2 + c_2 \sum_{k=0}^K \|w_k\|^2$ , which is only dependent on the disturbance and initial condition. Examining the relevant plots for both the H-form and V-form implementations confirm

this. As can be seen from Figure 6, the sum of squares of the states rises quickly at the beginning due to the effect of the initial condition, and the intermediate states where the system is approaching the origin. The plot then levels off considerably once the system states converge to a small region around the origin, and the slightly positive slope can then be explained by the  $c_2 \sum_{k=0}^K ||w_k||^2$  term from equation 90. The same effect can be seen for the V-form controller, with the levelling off effect occurring at a slightly higher value. Because the value of the sum of the states is partly dependent upon the disturbances, a random variable, the sum of states is also a random variable, thus this slightly different level between the H-form and V-form controllers is not enough to conclude that the H-form implementation has better performance, as running the simulations multiple times yields slightly different results, with the average tailing off value of each controller being roughly equal in the average.

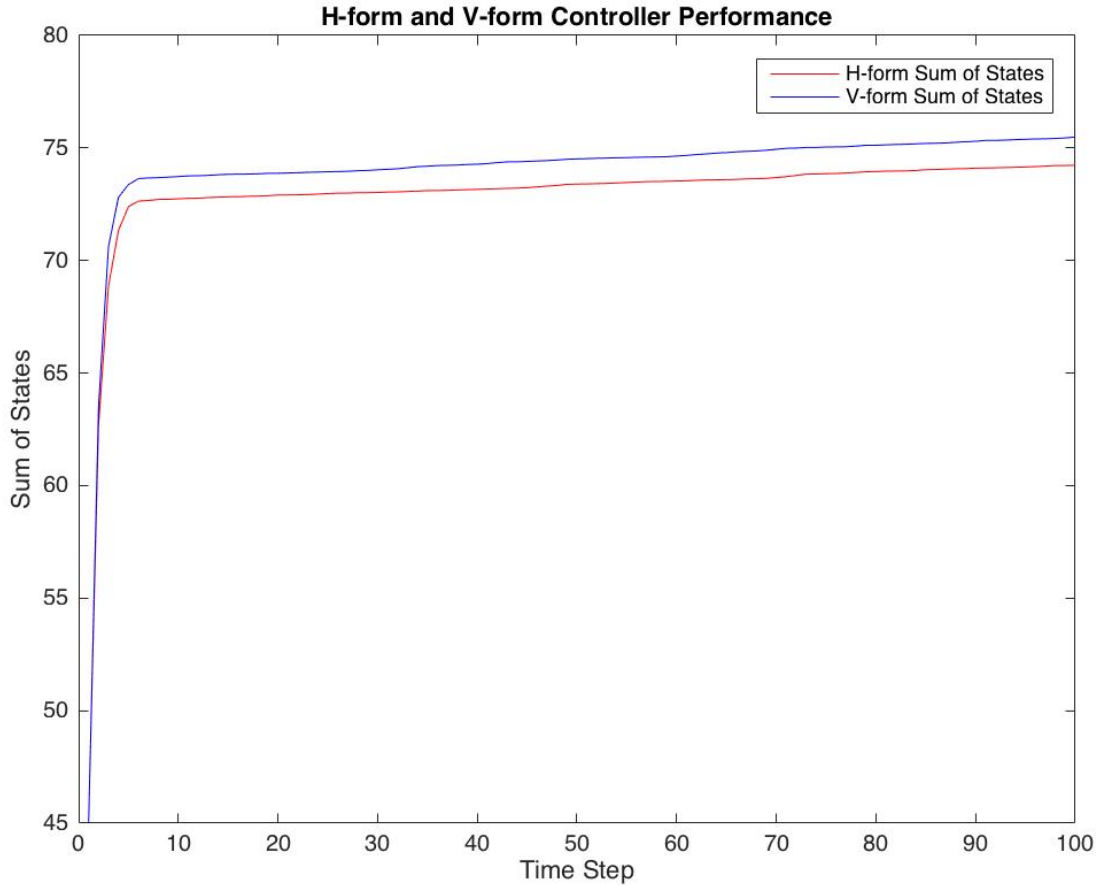


Figure 6: Sum of square of states: H-Form and V-Form. As the sum of states squared is a random variable, the small difference between H-form and V-form controller is not enough to determine which controller displays better performance.

Both implementations were simulated in Matlab, and both algorithms were programmed with YALMIP and Gurobi [12], [13]. YALMIP (yet another LMI parser) is a tool that can be used to

solve optimisations problems frequently occurring in systems and control theory. YALMIP is able to automatically detect what kind of optimisation problem that the user has defined, and then chooses the suitable solver to solve the optimisation problem. If there is not a suitable solver present for the type of optimisation problem defined, YALMIP will attempt to convert the optimisation problem to a form for which an appropriate solver exists [12]. In the H-form implementation, the solver used is Gurobi which can be used for linear programming and quadratic programming applications. The V-form algorithm is slightly more complex in that the online optimisation constraints include linear matrix inequalities (LMIs), which makes the problem a semi-definite programming (SDP) problem, and thus Gurobi cannot be used for the V-form implementation. The SDP solver used in the V-form implementation is MOSEK [14].

## 6.5 Improvements on Existing Algorithms

The algorithms discussed up to this point in this report are either recreations of algorithms existing in the current literature, or recreations of these algorithms with slightly different implementations. The H-form algorithm stated in previous sections is a recreation of the work of Lu and Cannon [1], and while the equivalent V-form implementation of the algorithm has not been seen in literature, it is the equivalent of algorithms that have been published.

It is to be expected that implementing a persistent excitation condition that not only accounts for previous and current time steps, but also for future time steps will increase the rate of convergence of the parameter set estimate. This technique has not been seen in the context of robust adaptive MPC, and it is therefore a novel contribution to the field. The results of implementing such a condition are discussed and examined in the next section.

Up to this point, all implementations have assumed that the current state is known perfectly, however in reality this will never be the case. One can allow for some degree of measurement uncertainty by including in the model an unknown time-varying random disturbance on the parameter. Thus in the next sections the author will consider a version of the previous algorithm where rather than the true parameter being an unknown constant, the true parameter value at a given time step lies within a bounded set containing the unknown true parameter value,  $\theta_k = \theta^* + \tilde{\theta}_k$ , where  $\tilde{\theta}_k \in S = \{\theta : U\theta \leq h\}$ .

### 6.5.1 Future Persistent Excitation Condition

As mentioned in previous sections, a persistent excitation condition accounting for past and present states is represented by the equation

$$\sum_{k=t-n}^t D(x_k, u_k)^T D(x_k, u_k) > \beta^2 I. \quad (91)$$

As mentioned earlier, this is a linear matrix inequality constraints which dictates the use of the solver MOSEK instead of Gurobi.

The idea leading to a persistent excitation condition with future time steps incorporated is a simple extension of the idea in equation 91; one must simply modify the upper limit of the summation to be  $t + N$  so that the summation includes future time steps:

$$\text{Future PE Condition: } \sum_{k=t-n}^{t+N-1} D(x_k, u_k)^T D(x_k, u_k) > \beta^2 I \quad (92)$$

Having extended the summation to future time steps, the obvious question that arises is the question of what values to use for  $x_k$  and  $u_k$  where  $k$  is in the future.

To implement this future PE condition, a convex sufficient condition for the PE condition is constructed using a linearisation process. Take an 'estimate' of the current state to be the actual value of the current state  $\hat{x}_0 = x_t$ . Estimates for future states can then be defined recursively by

$$\hat{x}_{k+1} = A(\hat{\theta})\hat{x}_k + B(\hat{\theta})\hat{u}_k, \quad (93)$$

where  $x_k \in X_k = \{x : Vx \leq \alpha_k\}$  and  $\hat{x}_k \in X_k$ . Thus  $x_k$  and  $u_k$  can be represented as the sum of an estimate term  $\hat{x}_k$  and  $\hat{u}_k$  respectively, and an error term  $\tilde{x}_k$  and  $\tilde{u}_k$ :  $x_k = \hat{x}_k + \tilde{x}_k$  and  $u_k = \hat{u}_k + \tilde{u}_k$ . Similarly to the estimate of  $x$ , the estimate for  $u$  is defined by the equation

$$\hat{u}_k = K\hat{x}_k + \hat{v}_k, \quad (94)$$

where the estimate for  $v$ ,  $\hat{v}$ , is the optimal predicted sequence for  $v$  computed at the last time step, shifted by one:  $\hat{v}_k = v_{k+1}^*$ . Having defined the estimates of  $x, u$ , and  $v$  in this way, the values of  $x_k$  and  $u_k$  to be used in future time steps of the PE condition are now fully defined. The reason for the future PE condition only being able to stretch  $N - 1$  time steps into the future as opposed to  $N$  steps into the future is due to the definition of  $\hat{v}$ . Because the optimal sequence for  $v$  calculated in the online optimisation is  $N$  elements long, where  $N$  is the prediction horizon length, taking the previously computed optimal sequence for  $v$  and shifting each element to the left by one step gets rid of the first element of  $v$  without replacing it with another element in the last time step, thus  $\hat{v}$  is  $N - 1$  elements long, meaning that both  $\hat{x}$  and  $\hat{u}$  are also defined to be  $N - 1$  elements long. From the definitions above, it is easy to show that  $\tilde{x}_k \in X_k - \{\hat{x}_k\}$  and  $\tilde{u}_k \in K(X_k - \{\hat{x}_k\}) + \{v_k\} - \{\hat{v}_k\}$ . Defining  $D(x_k, u_k)$  to be

$$D(x_k, u_k) = \begin{bmatrix} A_1 x_k + B_1 u_k & \dots & A_P x_k + B_P u_k \end{bmatrix}, \quad (95)$$

as in previous sections, one can write the following:

$$D(x_k, u_k) = D(\hat{x}_k + \tilde{x}_k, \hat{u}_k + \tilde{u}_k) = D(\hat{x}_k, \hat{u}_k) + D(\tilde{x}_k, \tilde{u}_k) \quad (96)$$

Following on from this, one can write:

$$\begin{aligned} D^T(x_k, u_k)D(x_k, u_k) &= D^T(\hat{x}_k, \hat{u}_k)D(\hat{x}_k, \hat{u}_k) \\ &\quad + D^T(\hat{x}_k, \hat{u}_k)D(\tilde{x}_k, \tilde{u}_k) \\ &\quad + D^T(\tilde{x}_k, \tilde{u}_k)D(\hat{x}_k, \hat{u}_k) \\ &\quad + D^T(\tilde{x}_k, \tilde{u}_k)D(\tilde{x}_k, \tilde{u}_k) \succeq \beta^2 I \end{aligned} \quad (97)$$

From similar arguments that were used in the discussion of the present time persistent excitation condition, because the last term in equation 97 is quadratic and necessarily positive definite, one can drop this term from the inequality to obtain an inequality that is sufficient for the future persistent excitation condition, but has a slight degree of conservativeness:

$$D^T(x_k, u_k)D(x_k, u_k) \geq D^T(\hat{x}_k, \hat{u}_k)D(\hat{x}_k, \hat{u}_k) + D^T(\hat{x}_k, \hat{u}_k)D(\tilde{x}_k, \tilde{u}_k) + D^T(\tilde{x}_k, \tilde{u}_k)D(\hat{x}_k, \hat{u}_k) \succeq \beta^2 I \quad (98)$$

Given that the vertices of the state tubes are known,  $X_k = \text{Co}\{U^j \alpha_k, j = 1, \dots, m\}$ ,  $D(\tilde{x}_k, \tilde{u}_k)$  can be written,

$$D(\tilde{x}_k, \tilde{u}_k) = D(\tilde{x}, K\tilde{x}_k + v_k - \hat{v}_k) \in \text{Co}\{D(U^j \alpha_k - \hat{x}_k, K(U^j \alpha_k - \hat{x}_k) + v_k - \hat{v}_k)\}. \quad (99)$$

Equation 98 then becomes

$$\begin{aligned} D^T(\hat{x}_k, \hat{u}_k)D(\hat{x}_k, \hat{u}_k) + D^T(\hat{x}_k, \hat{u}_k)D(U^j \alpha_k - \hat{x}_k, K(U^j \alpha_k - \hat{x}_k) + v_k - \hat{v}_k) + \\ D^T(U^j \alpha_k - \hat{x}_k, K(U^j \alpha_k - \hat{x}_k) + v_k - \hat{v}_k)D(\hat{x}_k, \hat{u}_k) \succeq \beta^2 I \end{aligned} \quad (100)$$

To implement this future persistent excitation condition, the following constraints must be added to the online optimisation problem.

$$\begin{aligned} \forall j : D_i^T(\hat{x}_i, \hat{u}_i)D_i(\hat{x}_i, \hat{u}_i) + D_i^T(\hat{x}_i, \hat{u}_i)D(U^j \alpha_k - \hat{x}_k, K(U^j \alpha_k - \hat{x}_k) + v_k - \hat{v}_k) + \\ D_i^T(U^j \alpha_k - \hat{x}_k, K(U^j \alpha_k - \hat{x}_k) + v_k - \hat{v}_k)D_i(\hat{x}_i, \hat{u}_i) \succeq M_i \\ M_i \geq 0 \\ \sum_{i=1}^{N-1} M_i \succeq \beta^2 I \end{aligned} \quad (101)$$

The above constraints are added for each  $i = 1, \dots, N - 1$ , so in total, imposing the future persistent excitation condition requires the inclusion of  $j \times (N - 1)$  ( $j$  is the number of vertices of the state tube) additional constraints to the online optimisation.

### 6.5.2 Varying True Model Parameter

The previous section detailed the implementation of a persistent excitation condition that stretched into future time steps, which is expected to speed up the convergence of the parameter set. This section will examine a new parameter set update algorithm that will allow the parameter set to still converge to a point  $\theta^*$ , when the true parameter value used at each time step is

$$\theta_k = \theta^* + \tilde{\theta}_k \quad \tilde{\theta}_k \in S = \{\theta : U\theta \leq h\}. \quad (102)$$

Using similar approaches to the derivation of the original parameter set update algorithm discussed in previous sections, one can begin by writing

$$x_{k+1} = A(\theta_k)x_k + B(\theta_k)u_k + w_k, \quad (103)$$

which can be expanded using the definition of  $A(\theta)$  and  $B(\theta)$  from equation 2 to be written as

$$x_{k+1} = \begin{bmatrix} A_0 & A_1[\theta_k]_1 & A_2[\theta_k]_2 & A_3[\theta_k]_3 \end{bmatrix} x_k + \begin{bmatrix} B_0 & B_1[\theta_k]_1 & B_2[\theta_k]_2 & B_3[\theta_k]_3 \end{bmatrix} u_k + w_k. \quad (104)$$

Separating the theta dependent terms from the non-theta dependent terms gives

$$\begin{aligned} x_{k+1} &= A_0x_k + B_0u_k + \begin{bmatrix} A_1x_k + B_1u_k & A_2x_k + B_2u_k & A_3x_k + B_3u_k \end{bmatrix} \theta_k + w_k \\ &= A_0x_k + B_0u_k + \begin{bmatrix} A_1x_k + B_1u_k & A_2x_k + B_2u_k & A_3x_k + B_3u_k \end{bmatrix} (\theta^* + \tilde{\theta}_k) + w_k. \end{aligned} \quad (105)$$

Using the definition of  $D(x_k, u_k)$  from equation 22, this gives

$$x_{k+1} = A_0x_k + B_0u_k + D(x_k, u_k)\theta^* + D(x_k, u_k)\tilde{\theta}_k + w_k. \quad (106)$$

The unfalsified parameter set at time  $k + 1$  can thus be written

$$\Delta_{k+1} = \{\theta^* : x_{k+1} - A_0x_k - B_0u_k - D(x_k, u_k)\theta^* = D(x_k, u_k)\tilde{\theta}_k + w_k\}, \quad (107)$$

and the updated parameter set is given by  $\Theta_{k+1} \supseteq \Theta_k \cap \Delta_{k+1}$  where  $\Theta_k = \{\theta : \Pi_\theta \theta \leq \pi_{\theta,k}\}$ . The

vector that defines the updated parameter set is computed from the optimisation problem below:

$$\begin{aligned}
[\pi_{\theta,k+1}]_i &= \max_{\theta^*, \tilde{\theta}, w} [\pi_{\theta}]_i \theta^* \\
\text{s.t. } & \Pi_{\theta} \theta^* \leq \pi_{\theta,k} \\
& x_{k+1} - A_0 x_k - B_0 u_k - D(x_k, u_k) \theta^* = D(x_k, u_k) \tilde{\theta} + w \\
& U \tilde{\theta} \leq h \\
& \Pi_w w \leq \pi_w
\end{aligned} \tag{108}$$

In the formulation above, we have defined  $\theta^* \in \hat{\Theta}_k$ , and  $\tilde{\theta} \in S$  where  $\hat{\Theta}_k = \{\theta : \Pi_{\theta} \theta \leq \pi_{\theta,k}\}$  and  $S = \{\theta : U \theta \leq h\}$ . Given these definitions for the sets that  $\theta^*$  and  $\tilde{\theta}$  lie in, the parameter  $\theta_k$  lies in a set defined by the Minkowski sum of the sets  $\hat{\Theta}_k$  and  $S$ :  $\Theta_k = \hat{\Theta}_k \oplus S$ , where the operator  $\oplus$  denotes the Minkowski sum. The Minkowski sum of two general polytopes is not straightforward to calculate, so to ease the computational burden of the algorithm, the sets that  $\theta^*$  and  $\tilde{\theta}$  lie in were defined to be similar, meaning that  $\theta^* \in \hat{\Theta}_k = \{\theta : \Pi_{\theta} \theta \leq \pi_{\theta,k}\}$  and  $\tilde{\theta} \in S = \{\theta : \Pi_{\theta} \theta \leq h\}$ . With the sets defined in this way, the set that  $\theta_k$  lies in can trivially be defined as the Minkowski sum of  $\hat{\Theta}$  and  $S$ :  $\theta_k \in \Theta_k = \hat{\Theta}_k \oplus S = \{\theta : \Pi_{\theta} \theta \leq \pi_{\theta,k} + h\}$ .

Because the definition of the set that  $\theta_k$  lies in has been modified slightly, a slight change in the constraints to the online optimisation is also required to implement the new parameter set update algorithm. Specifically, the constraints

$$\begin{aligned}
\Lambda_{i|k}^j \pi_{\theta,k} &\leq \alpha_{i+1|k} - Vd(U^j \alpha_{i|k}, KU^j \alpha_{i|k} + v_{i|k}) - \bar{w} \\
\Lambda_{N|k}^j \pi_{\theta,k} &\leq \alpha_{N|k} - Vd(U^j \alpha_{N|k}, KU^j \alpha_{N|k}) - \bar{w}
\end{aligned} \tag{109}$$

must be rewritten as

$$\begin{aligned}
\Lambda_{i|k}^j (\pi_{\theta,k} + h) &\leq \alpha_{i+1|k} - Vd(U^j \alpha_{i|k}, KU^j \alpha_{i|k} + v_{i|k}) - \bar{w} \\
\Lambda_{N|k}^j (\pi_{\theta,k} + h) &\leq \alpha_{N|k} - Vd(U^j \alpha_{N|k}, KU^j \alpha_{N|k}) - \bar{w}.
\end{aligned} \tag{110}$$

This is a slight modification to the online optimisation proposed in previous sections, but it is necessary for the online optimisation to work correctly together with the newly proposed parameter set update algorithm.

Following along the lines of the discussion about the distribution of the disturbance and its relation to the rate of convergence of the parameter set estimate, one can make similar arguments about the value chosen at each time step for  $\tilde{\theta}$ . Much like the disturbance set argument, the rate of convergence of the parameter set will now also be dependent upon how often the value for  $\tilde{\theta}$  lies on the boundary



of the set it is contained in  $S$ . The more often that  $\tilde{\theta}$  lies on the boundary of  $S$ , the quicker the parameter set estimate will converge to  $\theta^*$ , and the less often  $\tilde{\theta}$  lies on the boundary of  $S$ , the slower the parameter set estimate will converge.

In the simulations performed utilising the newly proposed parameter set update algorithm, both the disturbance and value for  $\tilde{\theta}$  were chosen to lie on the boundaries of their respective sets to speed up parameter set convergence and lessen the simulation time required.

It is conjectured that the rate of parameter set convergence will be slower in the newly proposed algorithm with uncertainty on the true parameter value because the total uncertainty in the overall system has risen. The numerical results achieved from performing these simulations, and the simulations including the persistent excitation constraint that stretches into future time steps will be presented in the next section.

## 7 Results and Discussion

This section will examine the numerical results achieved from simulating controllers with two novel qualities discussed in the previous section. Both of the novel algorithms described are implemented as part of the V-form implementation. In order to implement the future PE condition, the vertices of the state tubes must be known, which necessitates the use of the V-form algorithm. While the new parameter set update algorithm can theoretically be used in conjunction with both the H-form and V-form algorithms, the numerical results displayed below were obtained from using the algorithm together with the V-form implementation.

The specific numerical example used in these simulations is the same as the numerical example from Cannon and Lu's paper, and from previous sections. The prediction horizon used was 10 time steps long ( $N = 10$ ), and the simulation was programmed in Matlab using YALMIP and the semidefinite programming solver MOSEK.

### 7.1 Future PE Condition

Simulation results from the specific numerical example being examined has confirmed intuition that the inclusion of a persistent excitation condition that takes into account future time steps will increase the rate of convergence of the parameter set estimate. As Figure 7 shows that while the states do approach the origin, the region around the origin to which the states eventually converge is a much larger region than seen before without the future PE condition. It is important to note that the inclusion of the  $-\lambda\beta^2$  in the cost function from equation 84 means that there are no longer any hard guarantees on the stability of the controller, but in practice while the states did not converge to a

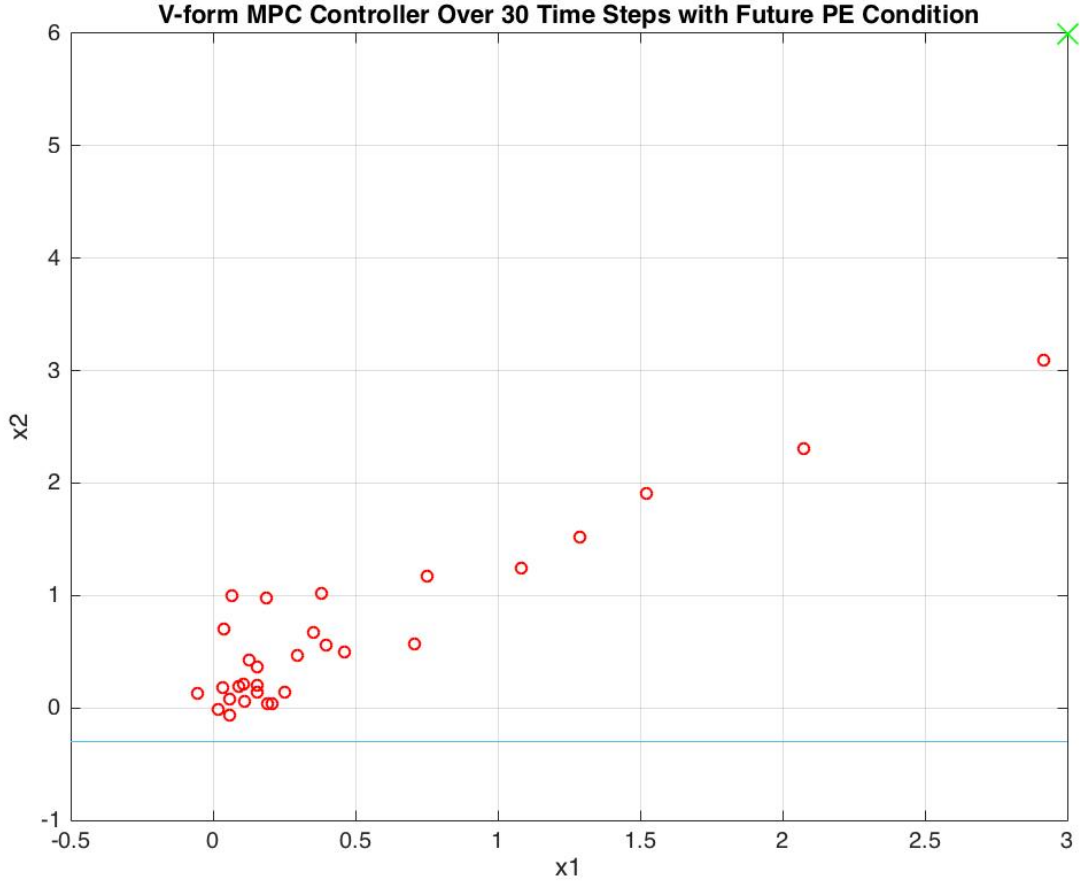


Figure 7: Evolution of states: V-form controller with future PE condition. The system state "explores" the state space, in the meantime gaining informative data about the parameter set.

tight region around the origin, they did appear to be bounded by a larger region around the origin. Figure 7 makes clear a trade-off between how closely the system tracks the reference (origin in this case), and how much new information is gained about the parameter set at each time step. In this example, because the system is allowed to 'explore' the state space more than the previous numerical example without a future PE condition, the system is able to identify the true value of the parameter quicker, and thus the parameter set estimate converges quicker than before.

Because the system does not converge to a small region around the origin, the plot of the sum of the squared states does not look as it does in previous examples. Whereas in previous examples the plot levels off at a point where it has a very shallow slope proportional to the sum of the squared disturbances thereafter, the sum of the squared states with the future PE condition imposed has clear sections where the sum rises quickly, meaning that there is not a prolonged section of shallow slope. This is evident from Figure 8. As can be seen, the sharp increase of the sum around time steps 18-23 correspond to the system states being further from the origin and 'exploring' the state space. This has the effect of increasing the information gained at each time step about the true parameter value,

directly leading to quicker convergence of the parameter set. Over the long run, this will eventually lead to better overall performance as having a more accurate parameter set estimate lowers the optimal cost and thus increases performance of the controller. Thus, in the short term, the controller performs slightly worse while the system is exploring the state space and acquiring new information about the model parameters which eventually translates into better performance.

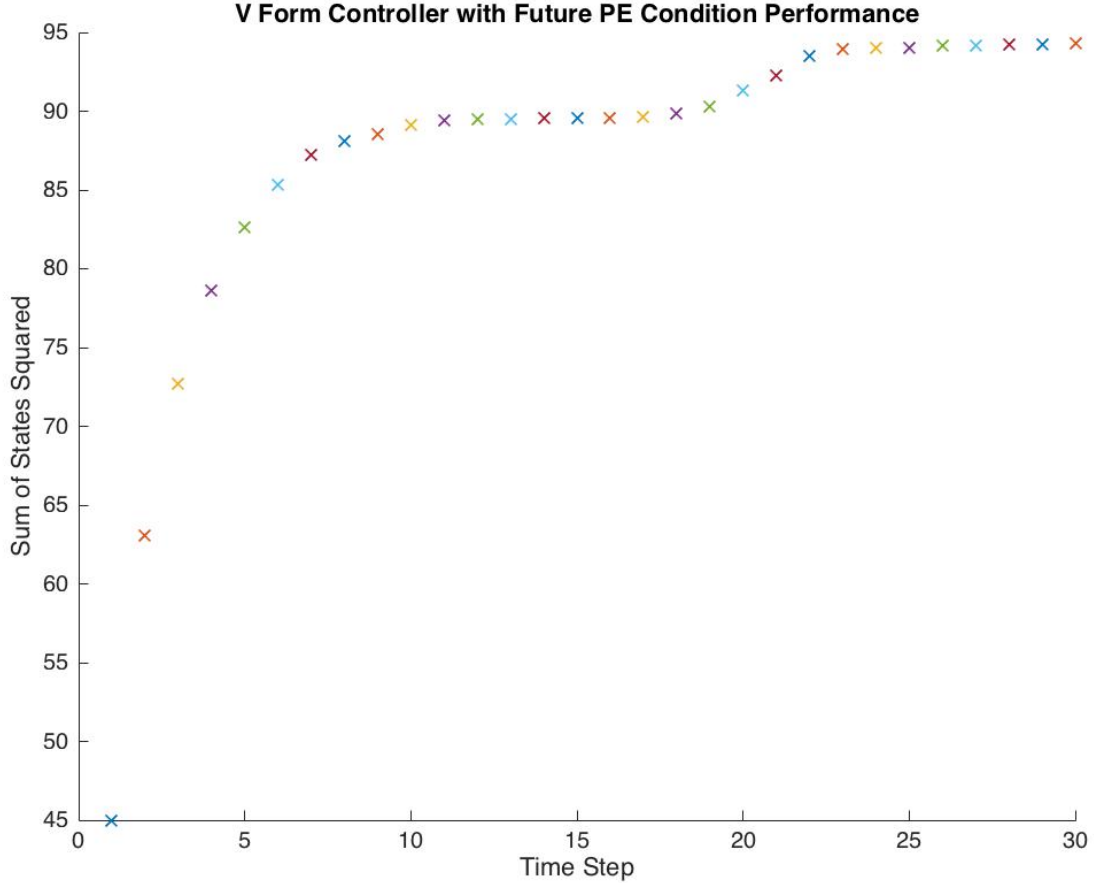


Figure 8: Sum of square of states: V-Form with Future PE condition. The rise in the graph around time step 20 is due to the system state deviating from the origin and exploring the state space, as can be seen from Figure 7.

With this argument in mind, an algorithm that selectively implements the future persistent excitation condition at specific time steps rather than implementing it constantly at every time step was proposed. In this way, the future PE constraint can be turned off in periods where the short term performance of the controller is most important, and in periods when the tracking of the controller can be relaxed, the future persistent excitation condition can again be implemented so that the controller is learning about the true parameter at a faster rate. This is an effective way to handle the trade off between close tracking of the reference, and fast parameter set estimate convergence. The two methods that the author has considered are the case when the future persistent excitation

condition is implemented on every other time step, and the case where it is implemented constantly over the first half of the simulation and then not over the second half of the simulation. Both of these proposed methods for handling the trade-off between controller performance led to quicker parameter set convergence compared to simulations when the persistent excitation condition only accounted for past and present time steps. Table 1 shows the final parameter set diameter after 60 time steps of each proposed method of implementing the persistent excitation condition over the course of ten separate simulations. The table clearly shows that both proposed methods of implementing the future

<b>Alternating Future PE</b>	<b>Future PE First 30</b>	<b>Present Time PE</b>
0.4392	0.1427	0.6999
0.1026	0.1366	0.4968
0.0370	0.6735	0.5280
0.0617	0.0971	0.2612
0.2460	0.0317	0.4197
0.5001	0.2429	0.3026
0.1368	0.2714	0.4486
0.1763	0.0165	0.0969
0.3278	0.1033	0.3519
0.2731	0.0413	0.3471
average = 0.23006	average = 0.1757	average = 0.39527

Table 1: Parameter Set Estimate Diameter After 60 Time Steps

persistent excitation condition result in significantly quicker parameter set convergence compared to the a persistent excitation condition considering only past time steps. While implementing the future persistent excitation constantly over the first half of the simulation achieved faster parameter set convergence than implementing the condition at alternating time steps over the length of the whole simulation, the states track the origin much closer when the future PE condition is implemented at alternating time steps, which is consistent with the arguments made previously.

Figure 9 shows the evolution of the system states over 60 time steps for the implementation where the future persistent excitation condition is enforced at every other time step over the entire length of the simulation time. The points plotted in blue correspond to time steps where the future PE condition was not enforced, and the red points correspond to time steps where the future PE condition was enforced. It can be seen that the states do not converge to a region around the origin that is as tight as the implementation that does not include a future persistent excitation condition, such as that showing in Figure 4, but it also tracks the origin much closer than a system that blindly implements the future persistent excitation condition at every time step.

Figure 10 shows the evolution of states of a controller that implements the future persistent excitation condition for the first thirty time steps then has no persistent excitation condition for the

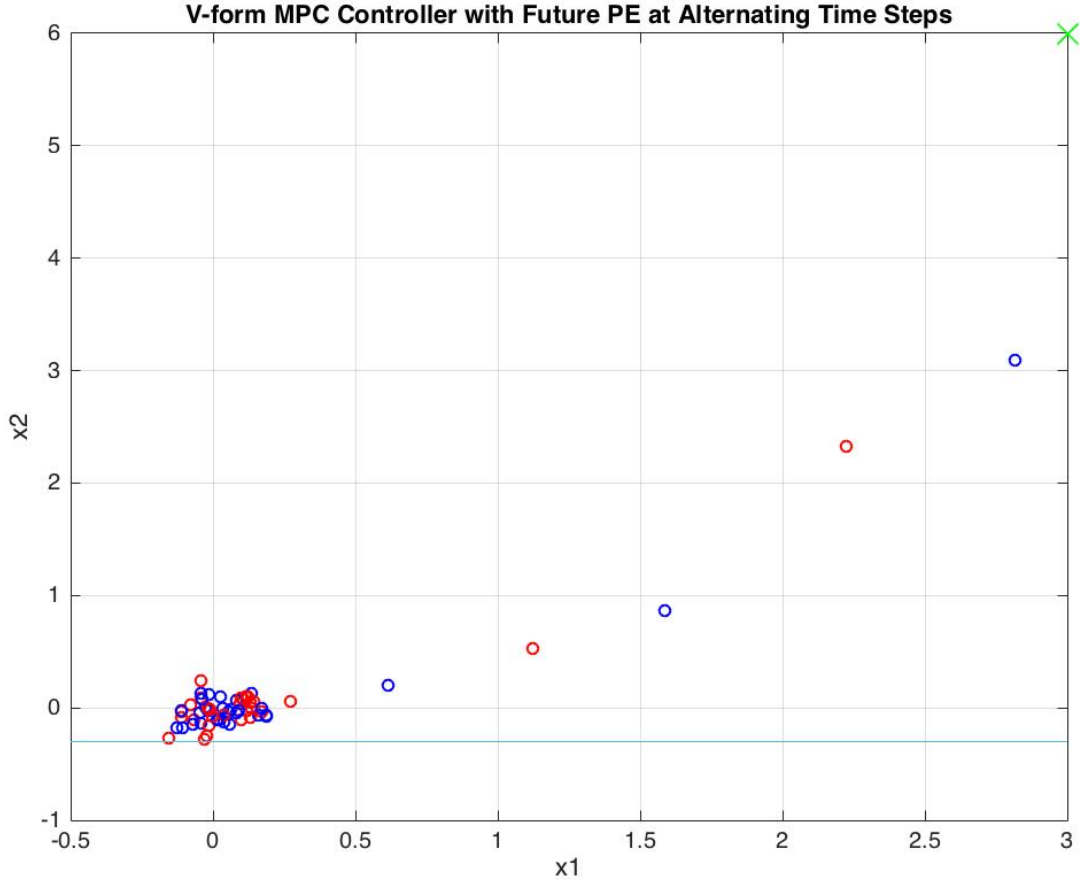


Figure 9: Evolution of States: V-form controller with Future PE condition at every other time step. Implementing the future PE condition at every other step allows the parameter set estimate to converge quicker while still converging to a region around the origin.

remaining thirty time steps. For the last thirty time steps, the future PE constraints are removed and the weight  $\lambda$  in the cost function is set to zero so that the objective function being optimised is the original nominal cost function discussed in prior sections, meaning the stability guarantees of the controller are recovered.

The red points in the graph respond to the first thirty time steps, where the future PE condition is being implemented and the blue points correspond to the final thirty time steps with no persistent excitation condition. The red points resemble the plot in Figure 7 as it is essentially the same simulation over the course of thirty time steps, and then the blue points resemble close the plot from Figure 4. The plot is as one would expect: in the first thirty time steps the system explores the state space more freely whilst quickly learning about the true model parameter and then the system is fully stabilised and tracks a region very tight around the origin once the future persistent excitation condition is turned off.

Plots of the sum of squared states of both simulations in Figure 11 further highlights the trade-off

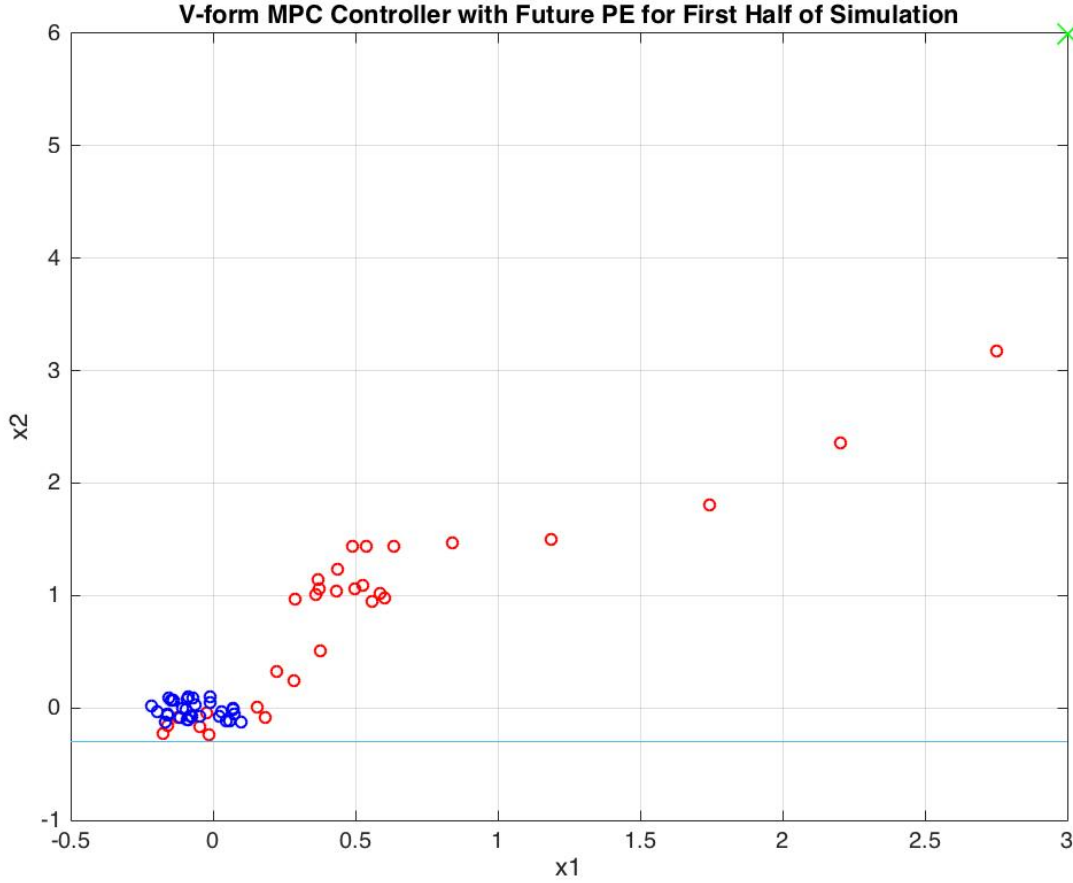


Figure 10: Evolution of States: V-form controller with Future PE condition for first 30 time steps. Another proposed method to increase parameter set convergence while still tracking the origin well.

between short term performance and speed of convergence of the parameter set estimate. It is clear to see that the short term performance of the controller that implements the future PE condition at alternating time steps is much better than the controller that implements the future PE condition for the first thirty time steps then no PE condition for the final thirty time steps, as evidenced by the much lower values of sum of squared states for the alternating future PE controller. This is completely in line with what would be expected as the plots of system states show that the alternating future PE system tracks the origin much more closely over the entire time range of the simulation compared to the system that implements the future PE condition for the first half of the simulation. As a result, one would expect the plot of the sum of squared states of the alternating future PE condition controller to have lower values to its counterpart. However, due to the trade-off discussed, and as the table clearly shows, the alternating future PE condition controller does not exhibit parameter set convergence that is as quick as its counterpart.

As the trade-off between parameter set convergence rate and short term performance is made clear, and obvious question that arises is how to effectively strike a balance between two competing effects.

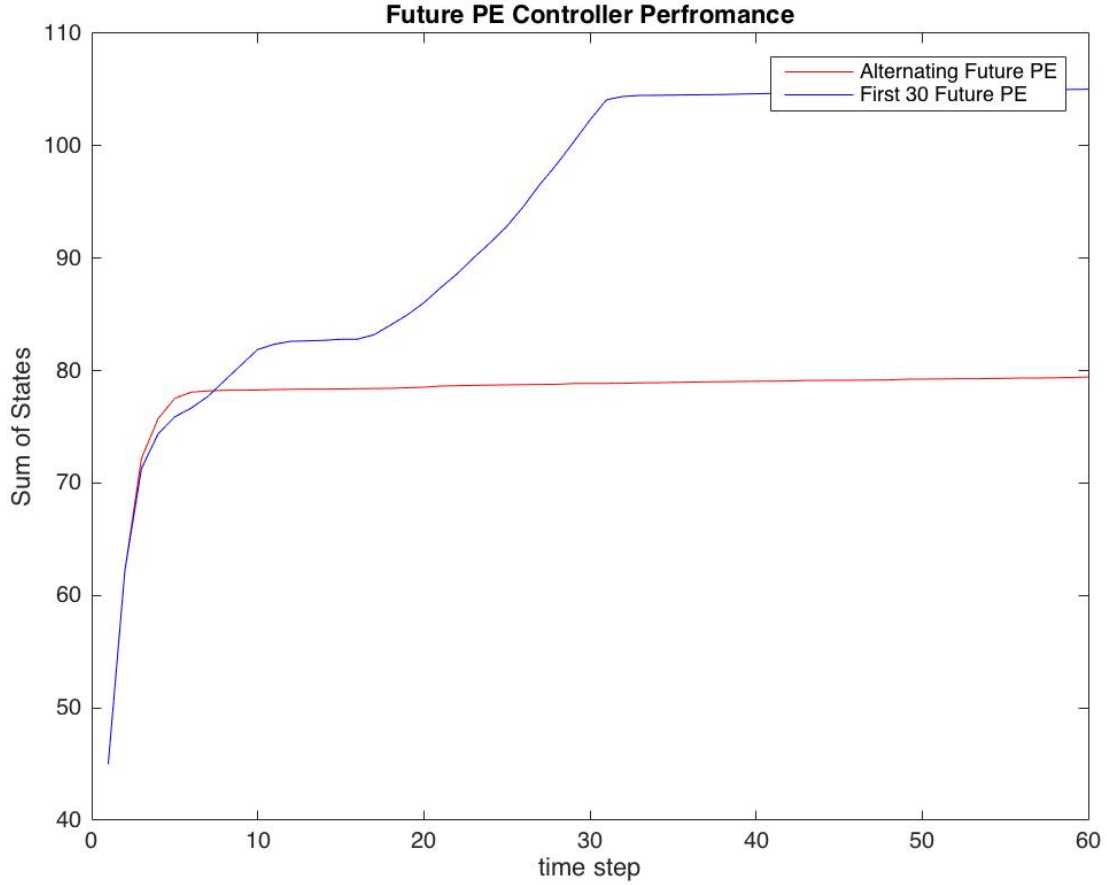


Figure 11: Performance of V-form Controller with future PE condition at every other time step and with Future PE for first half of simulation

As the parameter set converges to a singleton at the true parameter value, the long term performance of the controller improves and the optimal cost decreases. Thus the trade-off is between long term high performance and short term high performance. Two possible methods are proposed here to balance this trade-off: alternate between implementing the future persistent excitation condition and no persistent excitation condition at every other time step, and implement the future persistent excitation condition constantly for a short period of time so that the parameter set greatly decreases in size, then turn the condition off so that the system is able to track the reference well. Essentially, the user of the controller must define periods where model identification is more important than reference tracking, and periods where the opposite is true, and then implement the future persistent excitation condition within these time periods accordingly. The two proposed methods are believed to be adequate general approaches that will work in most simple scenarios, but more work needs to be done on the topic.

Future work will consider using neural networks to intelligently choose when to apply the future persistent excitation condition, and when to not include a persistent excitation condition and prioritise reference tracking instead.

## 7.2 Varying True Model Parameter

It is important to still be able to recover the true parameter value in scenarios where at each time step there is a disturbance added to the true parameter value:  $\theta_k = \theta^* + \tilde{\theta}_k$  where  $\tilde{\theta}_k \in S = \{\theta : U\theta \leq h\}$ . The  $\tilde{\theta}$  term is included as a modelling assumption that allows for state and input dependent disturbances. Due to reasons discussed in the previous section, the matrix  $U$  defining the shape of the set  $S$  is defined to be equal to the matrix defining the shape of the parameter set estimate  $\Pi_\theta$ . This is so that the computation required to compute the Minkowski sum of the two sets is straightforward.

The objective of the newly proposed parameter set estimate update algorithm is to thus update the parameter set estimate so that it converges to a singleton containing the value of  $\theta^*$ . Following on from similar arguments made in the section discussing the convergence of the original parameter set estimate, it is possible for the new parameter set estimate algorithm to converge to a singleton containing  $\theta^*$  if there is a non zero probability of the value of  $\tilde{\theta}$  lying on the boundary of the set  $S$  and there is also a non-zero probability of the disturbance lying on the boundary of its set  $W$ . Again, the rate of convergence of the parameter set estimate will be dependent upon the distribution for the disturbance and  $\tilde{\theta}$  near the boundaries of their sets. If these values lie on the boundary of their respective sets often, convergence will be quick, and vice versa. To lower the simulation time required to observe convergence of the parameter set to  $\theta^*$ , the values for both  $\tilde{\theta}$  and the disturbance  $w_k$  were chosen to be on the boundaries of their respective bounding sets at each time step of the simulation.

Figure 12 below shows the diameter of the parameter set at each time step in a simulation over the course of 2000 time steps. As can be seen, the plot clearly shows that the parameter set estimate converges to a singleton, and the simulation confirms that this singleton contains the value of  $\theta^*$ . This numerically confirms the analysis that showed that the parameter set would converge to a singleton containing  $\theta^*$ . The reason that the parameter set converges to a single point in this simulation is because the bound on the disturbance on the parameter value is known exactly, i.e the set description  $\tilde{\theta} \in S = \{\theta : \Pi_\theta \theta \leq h\}$  is correct. In other words, the true disturbance in the simulation is also sampled randomly from the same set  $S$ . The randomly sampled disturbance is then projected onto the boundary of the set  $S$  to speed up the convergence of the parameter set estimate, but a guarantee of convergence still holds if this is not the case because the probability of the disturbance being on the boundary of the set  $S$  is non zero.

The discussion above has considered the case where the set  $S$  that the disturbance on the system parameter lies in is known exactly. In this case, as shown above, the parameter set estimate converges to the true value  $\theta^*$ . However, this case is very restricted and not likely to be satisfied in reality. The case where the only information known about the set  $S$  is an estimate of the set  $\hat{S}$  with the condition



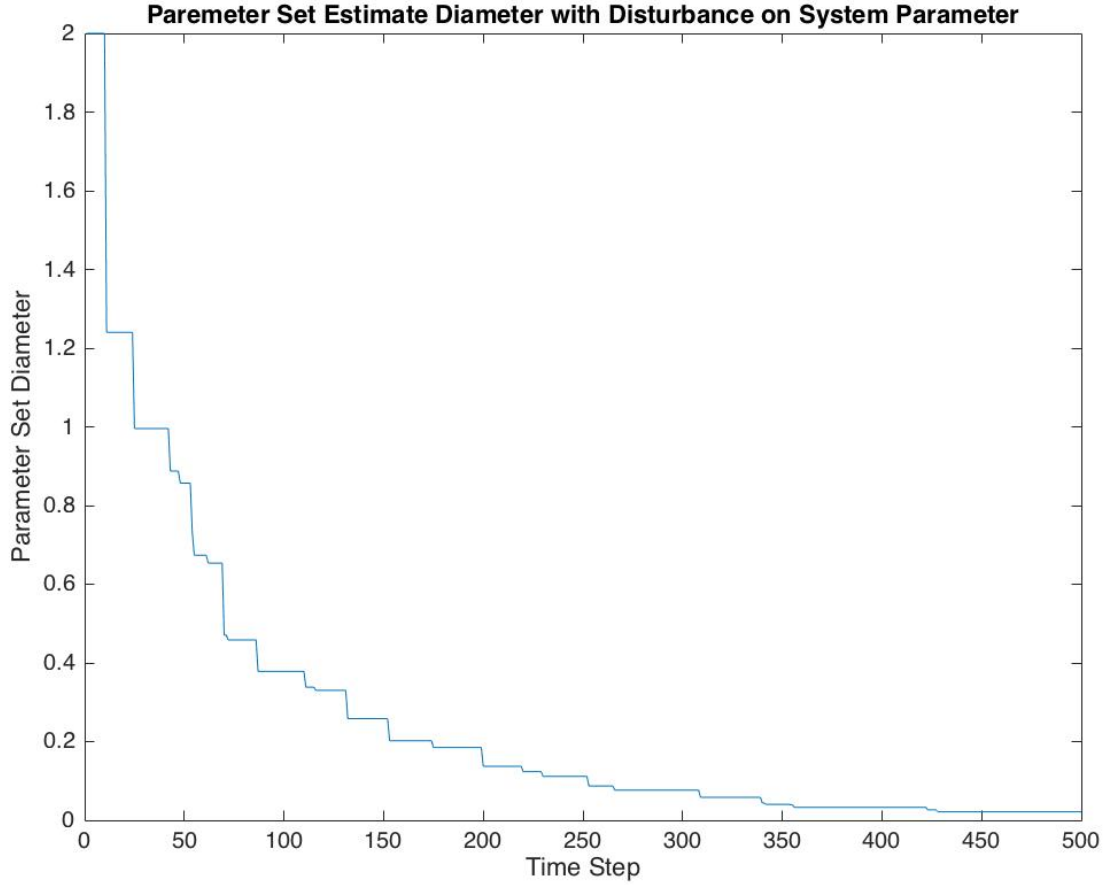


Figure 12: Diameter of the parameter set estimate when the system parameter takes the form  $\theta_k = \theta^* + \tilde{\theta}$

that  $\hat{S} \supset S$  is also examined. It would be a useful result to be able to show that  $\Theta_k \rightarrow \theta^* \oplus (\hat{S} \ominus S)$  as  $k \rightarrow \infty$ . The proof that this is indeed the case is shown below.

To begin the proof, it is important to show the proof of convergence of the parameter set to the true value of theta when there is no disturbance on the parameter, and the disturbance on the system lies within a bounded set ( $w_k \in W$ ).

$$\begin{aligned}
 x_{k+1} &= A(\theta^*)x_k + B(\theta^*)u_k + w_k \\
 &= D(x_k, u_k)\theta^* + d(x_k, u_k) + w_k \\
 &= D_k\theta^* + d_k + w_k, \quad w_k \in W
 \end{aligned} \tag{111}$$

The unfalsified parameter set is written as

$$\begin{aligned}
 \Delta_{k+1} &= \{\theta : x_{k+1} - D_k\theta - d_k \in W\} \\
 &= \{\theta : D_k(\theta^* - \theta) + w_k \in W\} \\
 &= \{\theta : D_k(\theta^* - \theta) \in W \oplus (-w_k)\}.
 \end{aligned} \tag{112}$$

Because there is an implementation of the future persistent excitation condition,  $\sum_{k=t}^{t+N-1} D_k^T D_k \geq \beta I$ , the following condition holds:  $\sum_{k=t}^{t+N-1} \|D_k(\theta^* - \theta)\|^2 \geq \beta \|\theta^* - \theta\|^2$ . This implies that  $D_k(\theta^* - \theta) \neq 0$  if  $\theta^* \neq \theta$ .

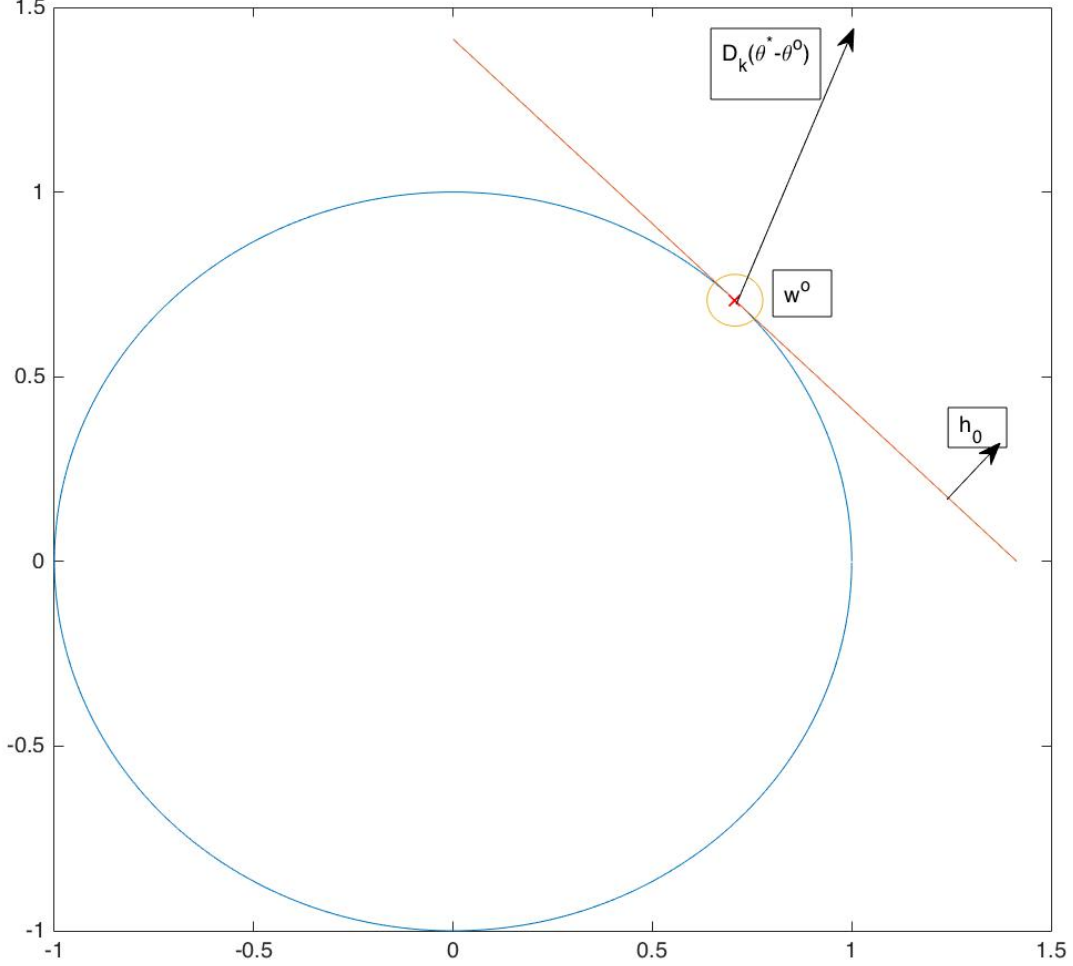


Figure 13:  $h_o^T D_k(\theta^* - \theta^e) \geq 0$

The condition for a particular value of  $\theta$ ,  $\theta^e$ , to be excluded from the unfalsified parameter set is  $h_o^T D_k(\theta^* - \theta^e) \geq 0$ , where  $h_o$  is the normal vector describing the hyperplane that is tangent to the disturbance set at a point  $w_o$ . This is demonstrated graphically in Figure 13. Thus for a realisation of the disturbance  $w_k$  that is arbitrarily close to the point  $w_o$ ,

$$\forall \epsilon > 0 \quad \Pr\{\|w_k - w_o\| < \epsilon\} > \delta \quad \text{for some } \delta > 0$$

$$\text{If } \|D_k(\theta^* - \theta^e)\| > \gamma$$

$$\text{Then } \theta^e \notin \Delta_{k+1} \Leftarrow \begin{cases} h_o^T D_k(\theta^* - \theta^e) > 0 \\ \text{If } \|w_k - w_o\| < \epsilon \end{cases} \quad (113)$$

where  $\gamma = \epsilon$ . As these conditions are satisfied with non zero probability, there is a non zero probability that a particular value of  $\theta^e \neq \theta^*$  will be excluded from the unfalsified parameter set, meaning that over an infinite period the parameter set will converge to a singleton at the true parameter value  $\theta^*$  with probability one.

For the case where the disturbance set  $W$  is not known exactly, but an estimate  $\hat{W}$  that is the smallest set that bounds  $W$  is known ( $\hat{W} \supset W$ ), the same arguments can be made to show convergence of the parameter set estimate if it is possible to define  $w_o$  as a point on the boundary of both  $W$  and  $\hat{W}$  (i.e. there must be points common to both boundaries).

$$\begin{aligned}\Delta_{k+1} &= \{\theta : D_k(\theta^* - \theta) + w_k \in \hat{W}\} \\ &= \{\theta : D_k(\theta^* - \theta) \in \hat{W} \oplus (-w_k)\}\end{aligned}\tag{114}$$

This equation is in the same form as the previous discussion, and the same arguments can be made to prove convergence of the parameter set estimate under these conditions.

For the more general case where  $\hat{W}$  is a conservative estimate of the disturbance set  $W$  such that  $\hat{W} = W \oplus \tilde{W}$ , one can again show convergence of the parameter set estimate to the true parameter value by writing

$$\Delta_{k+1} = \{\theta : D_k(\theta^* - \theta) \in W \oplus \tilde{W} \oplus (-w_k)\},\tag{115}$$

meaning that the condition for the exclusion of  $\theta^e$  is  $D_k(\theta^* - \theta^e) \oplus (-\tilde{W}) \not\subseteq W \oplus (-w_o)$ . Again, invoking previous arguments, this shows convergence of the parameter set to set with a radius that depends on the radius of  $\tilde{W}$  containing the true parameter value.

The final case to consider is when the system parameter contains a noisy term and only a conservative estimate of the set that the disturbance lies in is known:  $\theta_k = \theta^* + \tilde{\theta}_k$ ,  $\tilde{\theta}_k \in S$ ,  $\hat{S} \supset S$ . Again using similar arguments as before, one can write the unfalsified parameter set

$$\Delta_{k+1} = \{\theta : D_k(\theta^* - \theta) + w_k + D_k\tilde{\theta}_k \in W \oplus D_kS\},\tag{116}$$

where  $D_kS = \{z : z = D_k\tilde{\theta}, \tilde{\theta} \in S\}$ . Next, let  $v_k = w_k + D_k\tilde{\theta}_k$ ,  $v_k \in W \oplus D_kS$ , then

$$\Delta_{k+1} = \{\theta : D_k(\theta^* - \theta) \in W \oplus D_kS \oplus (-v_k)\},\tag{117}$$

where  $W \oplus D_kS = \{w + D_k\tilde{\theta}, w \in W, \tilde{\theta} \in S\}$ . If the sets  $\hat{S}$  and  $S$  are of the same form, i.e  $\hat{S} = \{\theta : \Pi_S\theta \leq \pi_{\hat{S}}\}$  and  $S = \{\theta : \Pi_S\theta \leq \pi_S\}$ , then  $\hat{S} = (\hat{S} \ominus S) \oplus S$ . Using this identity, the condition for inclusion of  $\theta^e$  in the unfalsified set is

$$\theta^e \in \Delta_{k+1} \text{ if } D_k(\theta^* - \theta^e) \oplus \{-D_k(\hat{S} \ominus S)\} \in (W \oplus D_k S) \oplus \{-v_k^o\}, \quad (118)$$

meaning that

$$\theta^e \notin \Delta_{k+1} \Leftarrow h_o^T [D_k(\theta^* - \theta^e) - D_k \tilde{\theta}] > 0 \quad \forall \quad \tilde{\theta} \in \hat{S} \ominus S \quad (119)$$

proving that the parameter set estimate converges to  $\theta^* \oplus (\hat{S} \ominus S)$  as  $k \rightarrow \infty$ .

Simulations on the numerical example discussed in previous sections have confirmed that the theoretical results obtained above do hold. To reduce convergence time, both the disturbance on the system and the disturbance on the model parameter were chosen to lie on a vertex of their respective sets. With these conditions, the parameter set estimate was found to converge to  $\Theta_k = \theta^* \oplus (\hat{S} - S)$  after nearly 4000 time steps. As the disturbances were chosen to optimise the rate of convergence, one can expect the rate of convergence to be much slower than in this numerical example, however the parameter set estimate will converge to  $\Theta_k = \theta^* \oplus (\hat{S} - S)$  with probability one over a sufficiently long window, as proved above.

## 8 Conclusions

This report has examined in detail adaptive robust MPC algorithms existing in the relevant literature and has recreated the results reported in the literature. The report discusses at great length the theory behind these adaptive robust MPC algorithms, examining both the tube based model predictive control algorithm, and the set based model identification methods used in conjunction with the MPC algorithms.

The report then moves on to discuss the persistent excitation condition required to guarantee that the set based model identification algorithm will yield a parameter set estimate that converges to a singleton at the true parameter value with probability one over the course of an infinite period of time. Conditions that affect the rate of parameter set estimate convergence are then discussed.

The report then presents a novel V-form algorithm that is a tractable equivalent of the H-form algorithm presented by Lu and Cannon [1] that has comparable performance. The motivation for developing an equivalent V-form algorithm was due to the need to know the vertices of the predicted state tubes when implementing an improved persistent excitation condition that considers a window starting at current time and extending into the future, using the predicted states and inputs. This newly presented future persistent excitation condition has not been seen in the relevant literature before, and is believed to be original work. The theory needed to implement the future persistent excitation condition is discussed, and the results of the implementation are presented. This novel

future persistent excitation condition leads to significantly faster parameter set convergence compared to implementations of traditional persistent excitation conditions at the expense of allowing the system to deviate from the reference signal to a greater extent than in the traditional persistent excitation condition implementation. Methods of implementing the future persistent excitation condition that still allow for faster parameter set convergence with tighter tracking of the reference signal are discussed, and the numerical results of these algorithms are presented, demonstrating greatly improved parameter set convergence rate compared to existing algorithms while still maintaining tight tracking of the reference signal.

Finally, the report proposes a novel parameter set estimate update algorithm in the case that the model parameter is based on a 'true' parameter in the presence of an additive disturbance on the parameter:  $\theta_k = \theta^* + \tilde{\theta}_k$ ,  $\tilde{\theta} \in S$ . The algorithm is able to correctly identify the true value of the model parameter  $\theta^*$  in the case where the set  $S$  is known exactly. Additionally, it is proved that in the case where only a conservative estimate  $\hat{S}$  of  $S$  is known where  $\hat{S} \supset S$ , the algorithm yields a parameter set estimate that converges to  $\Theta_k = \theta^* \oplus (\hat{S} \ominus S)$  as  $k \rightarrow \infty$ . This disturbance on the model parameter allows for the consideration of estimation or observation errors in the state, and is a novel method not seen before in the relevant literature.

Future work will consider different mechanisms to devise a point estimate for the model parameter. Choosing this point estimate through the use of neural networks will be considered, and the performance of this scheme will be compared to traditional methods for picking a point estimate. Furthermore, work will consider the definition of a metric that will allow for the direct comparison of methods that implement the future persistent excitation condition at different time steps so that the trade off between parameter set convergence and how closely the reference is tracked can be quantified and compared to other systems. Finally, more intelligent methods to choose at which time steps the future persistent excitation condition is implemented on will be examined.

## References

- [1] X. Lu, M. Cannon, 2019, 'Robust Adaptive Tube Model Predictive Control', *American Control Conference*. Philadelphia, 10-12 July 2019
- [2] D. Seborg, T. Edgar, D. Mellichamp, F. Doyle, 2011, *Process Dynamics and Control*. 3rd ed. New York: John Wiley & Sons.
- [3] M. Cannon, 2018, *Lecture 1: Model Predictive Control*, Lecture Notes, University of Oxford, delivered 22 October 2018.

- [4] M. Lorenzen, M. Cannon, F. Allgöwer, 2018, 'Robust MPC with recursive model update', *Automatica*
- [5] F. Blanchini and S. Miani, *Set-Theoretic Methods in Control*. Birkhauser Boston, 2008.
- [6] L. Chisci, A. Garulli, A. Vicino, and G. Zappa, "Block recursive parallelotopic bounding in set membership identification," *Automatica*, vol. 34, no. 1, pp. 15-22, 1998
- [7] S. M. Veres, H. Messaoud, and J. P. Norton, "Limited-complexity model-unfalsifying adaptive tracking-control," *International Journal of Control*, vol. 72, no. 15, pp. 1417-1426, 1999
- [8] B. Hassibi, A. H. Sayed, and T. Kailath. LMS is  $H^\infty$  optimal. In *Proceedings of the Conference on Decision and Control*, pg 74-79, vol. 1, 1993
- [9] E.W. Bai, H. Cho, and R. Tempo, "Convergence Properties of the Membership Set," *Automatica*, vol. 34, no. 10, pp 1245-1249, 1998
- [10] M. Lorenzen, F. Allgöwer, and M. Cannon, "Adaptive Model Predictive Control with Robust Constraint Satisfaction," *IFAC-PapersOnLine*, vol. 50, no. 1, pp. 3313-3318, 2017.
- [11] E. Abraham, *Modelling and Analysis of Hybrid Systems; Convex polyhedra*, Lecture Notes, RWTH Aachen University, delivered SS 2015.
- [12] J. Löfberg, "YALMIP : A Toolbox for Modeling and Optimization in MATLAB", *In Proceedings of the CACSD Conference*, 2004
- [13] Gurobi Optimization, LLC, "Gurobi Optimizer Reference Manual", 2018, <http://www.gurobi.com>
- [14] MOSEK ApS, "Installation", 2017, <https://docs.mosek.com/8.1/install/installation.html>